1

TRACOR

SOME GUIDELINES FOR SONAR BAFFLE DESIGNS

PROBLEM 1

CONTRACT NObsr-85185

INDEX NO. SF001-03-01, TASK 8100

Prepared for

The Bureau of Ships
Code 689B

by

Texas Research Associates
A Division of TRACOR, Inc.

March 30, 1962

TRACOR, INC.

1701 Guadalupe St. Austin 1, Texas GR6-6601

TRACOR

TRACOR, INC. 1701 Guadalupe St Austin I, Texas GR6-6601

SOME GUIDELINES FOR SONAR BAFFLE DESIGNS

PROBLEM 1

CONTRACT NObsr-85185

INDEX NO. SF001-03-01, TASK 8100

Prepared for

THE BUREAU OF SHIPS
CODE 689B

by

TEXAS RESEARCH ASSOCIATES
A DIVISION OF TRACOR, INC.

Work Performed by:

E. H. Batey

H. R. Courts

F. Goodrich, Jr.

J. D. Morell

W. C. Moyer, Jr.

E. A. Tucker

A. F. Wittenborn

Approved by:

A. F. Wittenborn
Vice President

TABLE OF CONTENTS

TRACOR, INC [illegible] Austin, Texas

SOME GUIDELINES FOR SONAR BAFFLE DESIGNS

Abstract

The problem of sonar baffle design is examined analytically by developing expressions for the total sound field behind a baffle as a result of diffraction around and transmission through a baffle. The total sound field can be calculated using a digital computer and includes the effects of a finite bandwidth source, a source which has a finite spatial distribution and the alteration of the actual spatial extent of the source by a sonar dome. A study of the effects of the transducer as an object of finite size on the sound field has not yet been concluded.

It is shown that the sound field behind the baffle can interact with the beam forming process. For the transducer-baffle arrangements now in use, this interaction can produce coherent noise signals both fore and aft. For active sonars this interaction results in spokes on a PPI presentation.

It is concluded that the problem of sound transmission through the baffle does not require further investigation until the diffraction effects have been established quantitatively. It is not necessary or practical to reduce transmission much below the diffracted noise levels, and this may be possible with materials now available.

Some additional promising investigations are also mentioned in this report.

TRACOR, INC. 1701 Guadalupe St Austin 1, Texas

SOME GUIDELINES FOR SONAR BAFFLE DESIGNS

1. INTRODUCTION

This report describes a study performed to generate guidelines for the design of sonar baffles. These guidelines have been derived from the results of an analysis of the interaction of sound waves with baffles and, to some extent, domes using reasonable, though somewhat simplified, analytical techniques. The approach which has been taken was chosen in order to obtain mathematical descriptions of baffle performance suitable for obtaining usable results without excessive numerical calculations.

The effects of the baffle and the dome on sonar system performance are considered independently in this report. The effect of the transducer as an object of finite size in the resultant noise field has not yet been considered, nor has a thorough analysis of the effect of baffle curvature been made. A more complete treatment of the baffle-dome-transducer complex, including interactions between them, is in progress under another problem assignment. This later, more rigorous treatment may make it possible to assign better numerical values to the various effects encountered in the baffle-dome-transducer complex.

The purpose of a sonar baffle is to acoustically shield the sonar transducer from objectionable noise sources, usually sources arising from the sonar platform as opposed to sources occurring naturally in the sea. In this report the ship's screws are considered as the major objectionable noise sources whenever a specific example is required.

The sonar baffle designer has two basic parameters at his disposal for accomplishing the task of discriminating against objectionable noise sources. One of these is the geometry of the

baffle and the other is the material, or materials, from which it is made. These two parameters can be used to minimize, respectively, the two fundamental shortcomings of a realistic baffle system, namely diffraction around and transmission through the baffle. A study to develop guidelines for baffle design can therefore be conveniently and usefully initiated by considering each of the two basic parameters separately, i.e., by considering as independent the diffraction around and the transmission through a baffle. This was the procedure used for this analysis.

Section 2 of this report contains a discussion of diffraction effects around a baffle, based on calculations performed by using the analytical technique described in Appendix 1. Section 2 also contains a discussion of baffle and dome transmission effects based on calculations performed by using the analytical technique described in Appendix 2. It will be noted that transmission effects include both attenuation studies through the baffle and transmission studies through a sonar dome.

In Section 3 a discussion is given of the effect of diffraction around and transmission through a baffle in terms of sonar equipment performance.

2. METHOD OF ANALYSIS

As is well known, sound diffracts around the edges of a baffle in much the same manner as light diffracts around the edges of an opaque obstruction.* The structure of the diffraction pattern is dependent upon the geometry of the baffle or obstruction and also dependent upon the spectrum and spatial distribution of the noise source. The intensity level at any point in the diffraction pattern is dependent upon the pattern structure and the intensity of the incident wave or waves.

Because of its symmetry, a disc baffle is the simplest to treat mathematically. The diffraction pattern resulting from the disc can be described qualitatively by considering the case of plane waves of a single frequency at normal incidence to the plane of the disc. The rotational symmetry of the disc produces an axially symmetric pattern on planes parallel to the disc. Several wavelengths behind the disc there will be a region of high intensity on the axis of the disc. This central bright spot is surrounded by concentric circles, in planes parallel to the disc, of low and high intensity. In the case of light waves this results in the familiar bright spot surrounded by alternating dark and bright rings. Figure 1 shows a measured diffraction pattern behind a circular disc baffle for acoustic waves. It should be noted that the spatial extent of the diffraction pattern does not normally coincide with the geometrical shadow of the baffle. This implies that wave acoustics must be used because ray theory does not apply to this situation.

Because sonar transducers are usually right cylinders, baffles which have a rectangular projection are of greater interest to this

---

*See, e.g., Jenkens, F. A. and White, H. E., Fundamentals of Optics, McGraw-Hill Book Co., New York (1957) p 359 ff. Primakoff, H., Klein, M. J., Keller, J. B., and Cartensen, E. L., "Diffraction of Sound Around a Circular Disk," Internal memorandum Columbia University; and Keller, J. B., Klein, M. J. and Primakoff, H., "The Acoustic Shielding Effect of Baffles," Columbia University, Division of War Research (1945).

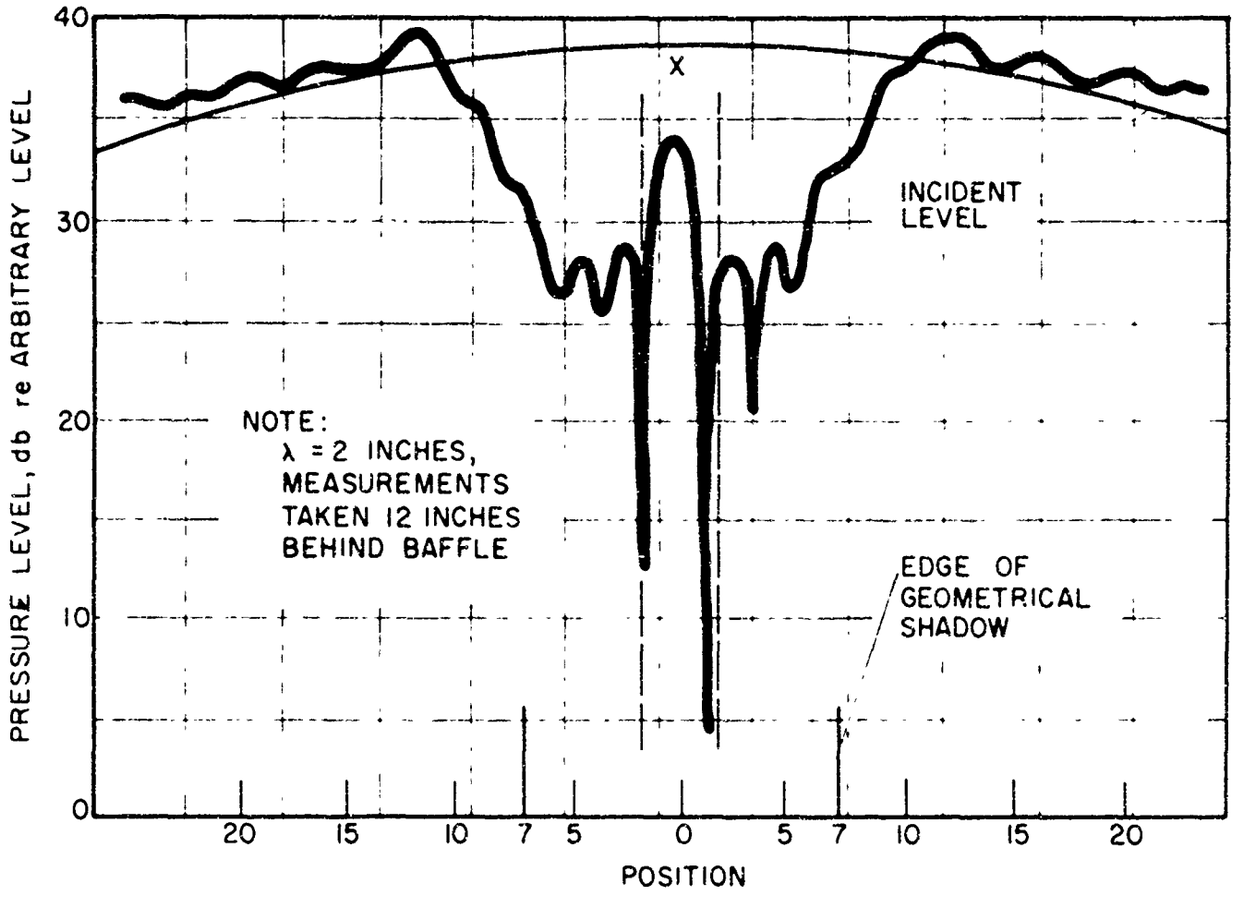

1

Fig. 1 - TYPICAL DIFFRACTION PATTERN BEHIND A DISK BAFFLE

TAKEN FROM THE ACOUSTIC SHIELDING EFFECT OF ACOUSTIC BAFFLES H PRIMAKOFF, J B KELLER & M J KLEIN

study than circular discs. In nearly all cases, sonar baffles are terminated at their upper and lower ends such that, for practical purposes, very little acoustic energy "leaks" around these edges. This would be the case, for example, for a baffle terminating on hull at its upper end and in a highly absorbing medium like a sand pack at its lower end. The net effect of these terminations is such that the rectangular baffle is approximately equivalent to an infinite strip baffle for ship's screw noise. This is the form that has been considered in the study described here.

A mathematical description of the diffraction pattern behind an infinite strip baffle is given in Appendix 1. The problem considered there is one in which the incident sound field is forced to remain a plane wave in front of and in the plane of the baffle. This is equivalent to the assumption that the front of the baffle is a perfect sound absorber. The rear of the baffle is likewise assumed to be a perfect absorber. Transmission through the baffle is considered to be independent of the diffraction phenomenon and is considered separately in the next section.

The diffracted sound field is formulated as a two dimensional function of position behind the baffle for an incident wave of single frequency from a point source at a specified angle of incidence. From this formulation realistic sound fields of finite bandwidth arising from spatially distributed sources can be treated by summation processes. A spatially distributed source can be considered as a number of elemental sources located at discrete angles chosen to approximate the spatial distribution of the source. A source of finite bandwidth can be treated, at each angle of incidence, as a number of elemental sources at a number of discrete frequencies chosen to approximate the frequency spectrum of the elemental source at a given angle of incidence. The total diffraction pattern can be obtained by summing the contribution of each

elemental source over both the finite bandwidth and the spatial extent of the source.

The presence of a sonar dome will have two effects on the sound field behind a baffle namely (1) it will attenuate the incident sound energy and (2) it will, because of its curvature, alter the spatial extent of the source as seen by the baffle. These effects are considered in some detail in Appendix 2. They can be accounted for quantitatively in estimating the total diffraction pattern. Normally the attenuation effects of the dome will be negligible in comparison with the baffle attenuation.

The effect of sound transmission through the baffle on the sound field behind a baffle is discussed in Appendix 2.2. It is concluded there that adequate mathematical descriptions of this effect are in existence, so that baffle absorption studies reduce primarily to a study of absorptive materials and geometry. For a given material, equations are given for estimating the transmission through a baffle so that this quantity can be added to the diffraction effects at each point in the sound field behind the baffle in order to obtain the total sound field.

All of the necessary calculations discussed above can be conveniently and rapidly carried out on a digital computer.

Figure 2 shows the diffraction patterns behind an infinite strip baffle computed for baffle width to wavelength ratios $(\frac{a}{\lambda})$ of 3.75, 4 and 5 for an acoustic sine wave incident normal to the baffle. The foreground of each photograph represents the plane of the baffle, while the successive planes looking into the picture represent the diffraction pattern at intervals of two wavelengths in planes parallel to the baffle. The relative intensities are shown on a linear scale. The shadow zone is in the center of each plane. Figure 3 shows the diffraction pattern behind an infinite strip baffle computed for a baffle width to wavelength ratio of 4 for an acoustic sine wave incident at 20° from the normal to the baffle.

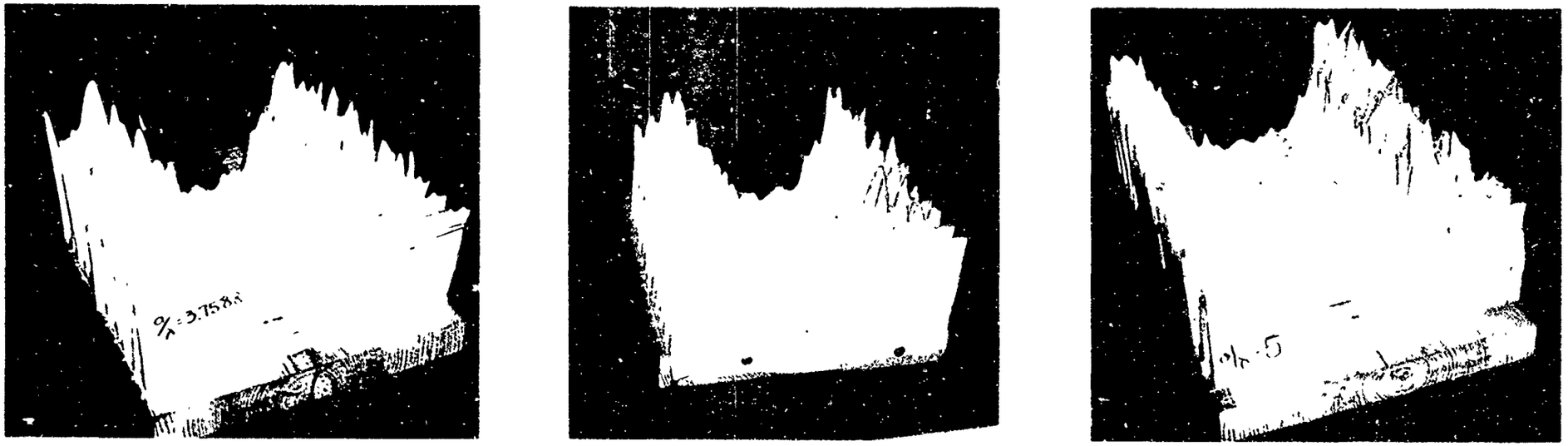

A. B. C.

Fig. 2 – DIFFRACTION PATTERN INTENSITY BEHIND AN INFINITE STRIP BAFFLE OF A NORMALLY-INCIDENT PLANE WAVE FOR THE INDICATED BAFFLE WIDTH TO WAVELENGTH RATIOS. (LINEAR SCALE)

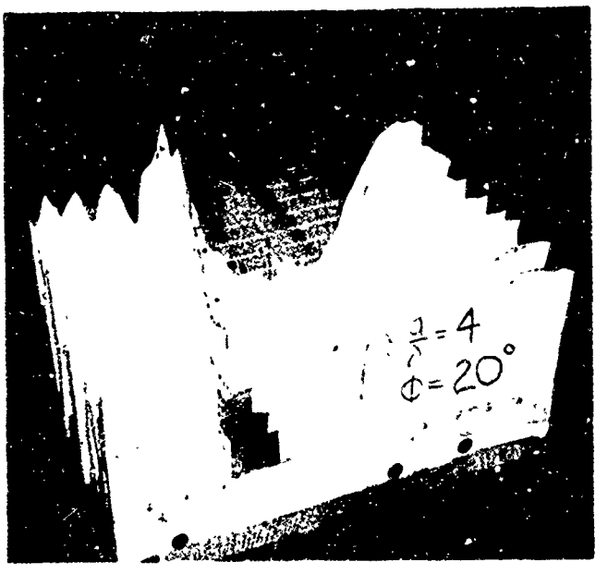

Fig. 3 - DIFFRACTION PATTERN INTENSITY BEHIND AN INFINITE STRIP BAFFLE OF A PLANE WAVE INCIDENT AT AN ANGLE OF 20° TO THE BAFFLE AXIS.

BAFFLE WIDTH TO INCIDENT WAVELENGTH RATIO IS 4. (LINEAR SCALE)

The structure of the diffraction pattern for the infinite strip is, as in the case of the disc, dependent on baffle geometry. However, instead of having the same intensity on any circle perpendicular to the baffle axis, one now has the same intensity on a line parallel with the baffle edge. As can be seen from Figures 2 and 3, the distribution of the intensity behind the baffle shows a central "bright" line with alternating "dark" and "bright" lines approximately parallel to the central one. In order to see the pattern in greater detail, the intensity distribution in a plane 18λ behind a strip baffle for a baffle width to wavelength ratio of 4 and normal incidence, is shown in Figure 4. This pattern corresponds to the pattern present in the vicinity of the transducer in a typical sonar installation. The central line is less intense, relatively, than the central spot for the disc. In an experimental measurement, the intensity minima shown in Figure 4 in the shadow zone would be obscured by transmission effects.

Figure 5 shows a linear scale comparison of the pattern given in Figure 4 to a measured pattern for light waves. The good correspondence between the two patterns indicates that the simplified boundary condition used in the diffraction calculations has no significant qualitative effect.

The effect of a source with a finite bandwidth will be to smooth the patterns shown in Figures 2 and 3 because the intensity maxima and minima from each portion of the incident spectrum will occur at different parts of the pattern. (This, of course, is not true for the central bright line.)

The effect of a source with a finite spatial distribution will be two-fold. First, the intensity maxima and minima will occupy different positions for different angles of incidence, so that the total pattern will become smoother. Secondly, the width of the region of relatively low intensity, i.e., the diffraction shadow zone, will be influenced. For normal incidence, it can be seen from Figure 2 that the shadow zone diverges slightly as a function

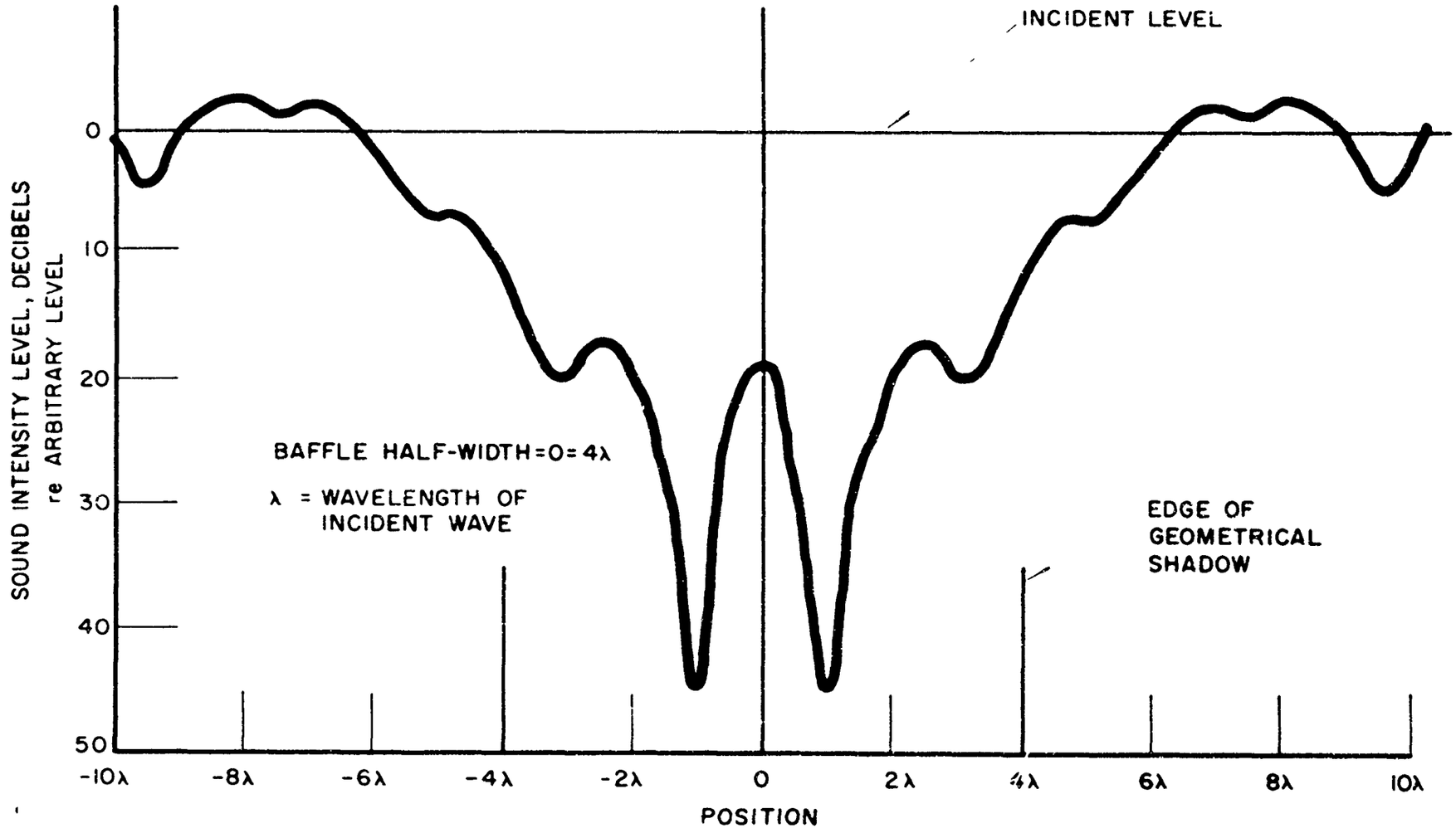

Fig. 4 — SOUND INTENSITY LEVEL AT A DISTANCE 18 λ BEHIND A STRIP

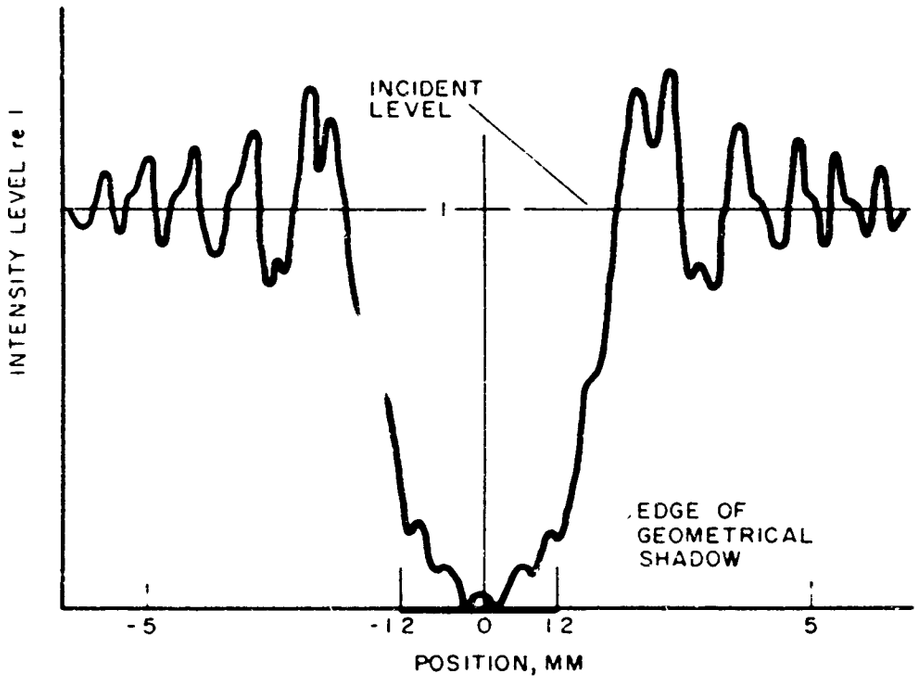

A. TYPICAL DIFFRACTION PATTERN BEHIND AN OPAQUE STRIP

TAKEN FROM FUNDAMENTALS OF CPTICS
F A JENKINS & H E WHITE

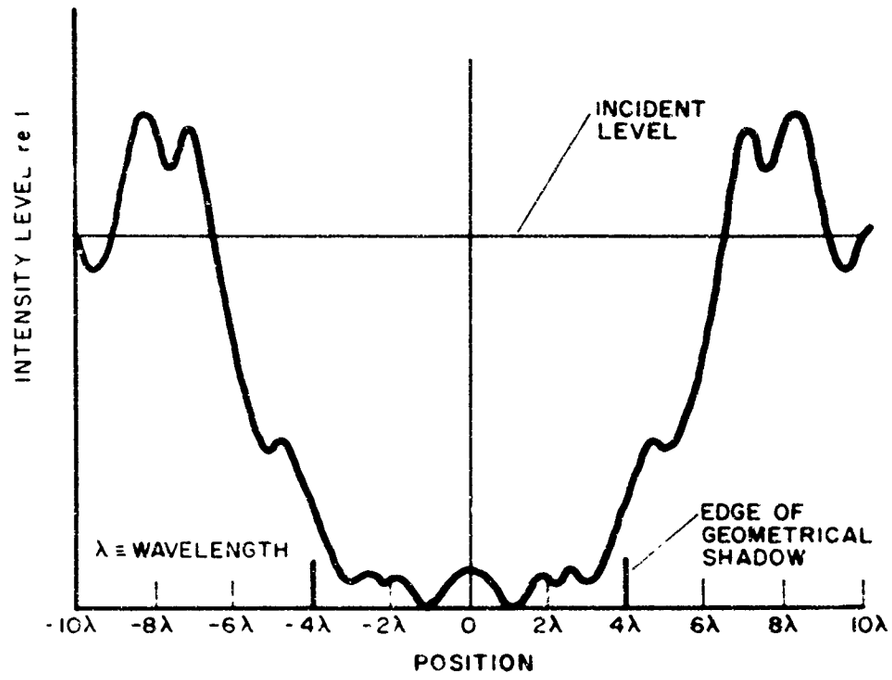

B. DIFFRACTION PATTERN 18 λ BEHIND AN INFINITE STRIP BAFFLE

Fig. 5

TRACOR, INC. DWG 2000-55
AUSTIN, TEXAS 5/18/62 AFW/JRR

of distance behind the baffle. For oblique incidence, the shadow zone also diverges, but the entire pattern is perpendicular to the plane of incidence, as can be seen from Figure 3. When a number of such patterns are summed the total effect will be to cause the pattern to converge, i.e., to become narrower as a function of distance from the baffle, and to broaden the region in which the average intensity rises from its low value in the shadow zone to the ambient value.

It should be noted that the intensity just outside the shadow zone will, in all cases, rise to a value greater than the intensity which would occur if the baffle were not present.

The discussion to this point has considered plane baffles. Although no quantitative calculations have been carried out, the following qualitative statements can be made concerning curved baffles. By considering the derivation of the equations giving the diffracted noise field behind the baffle (Appendix 1), it can be seen that small surface curvature has essentially no effect on the pattern. The important factor is the position of the baffle edges relative to the transducer, which will be discussed further below. The effect of the curved baffle on the transducer when it is used to transmit or receive, i.e., the lens effect of the curved baffle, has not yet been considered. Also the possibility of performing some "cute" tricks with multiple section baffles has not been, but should be explored. Smaller baffle sections located close to the transducer will not significantly alter the transmitted sonar pulse, but they might be used to alter the received diffracted noise field significantly.

3. DISCUSSION

As shown in Section 2, the total sound field behind a baffle taking into account the finite bandwidth of the source, the finite spatial extent of the source, the effect of the dome on modifying the actual spatial extent of the source, and transmission through the baffle, can be readily calculated using a digital computer. The manner in which this sound field is altered by the presence of the transducer is the subject of work presently in progress. It is of interest now to discuss the effect of the sound field behind the baffle on sonar system performance. Until the effect of the presence of the transducer is determined this discussion will remain qualitative. Nevertheless, as will be seen below, some interesting conclusions can be drawn.

Figure 6a shows a typical, smoothed, diffraction pattern which might be expected in a plane passing through the center of a transducer (without the transducer present) for an arrangement as shown in Figure 6b. (For an active sonar, with its relatively narrow pass band, the pattern will normally not be as smooth as it is shown in the figure, but this fact is not of great importance for the following discussion.) Consider a baffle, rectangular in projection such that the edges of the baffle are located at A and A'. Although it is possible that the baffle can be so wide that the entire transducer is within the region in which the intensity is less than the ambient from the objectionable noise source, such a situation does not usually occur in practice. The more common situation is the one depicted schematically in Figure 6b, where a portion of the transducer is in a low intensity field (the arcs B B' and C C') and a portion in a high intensity field (the arcs BC and B'C'). Normally the high intensity field will be greater than it would be if no baffle were present.

As stated above, the effect of the transducer as an object of finite size in modifying the diffraction pattern as computed here has not yet been determined. Nevertheless, it can be stated

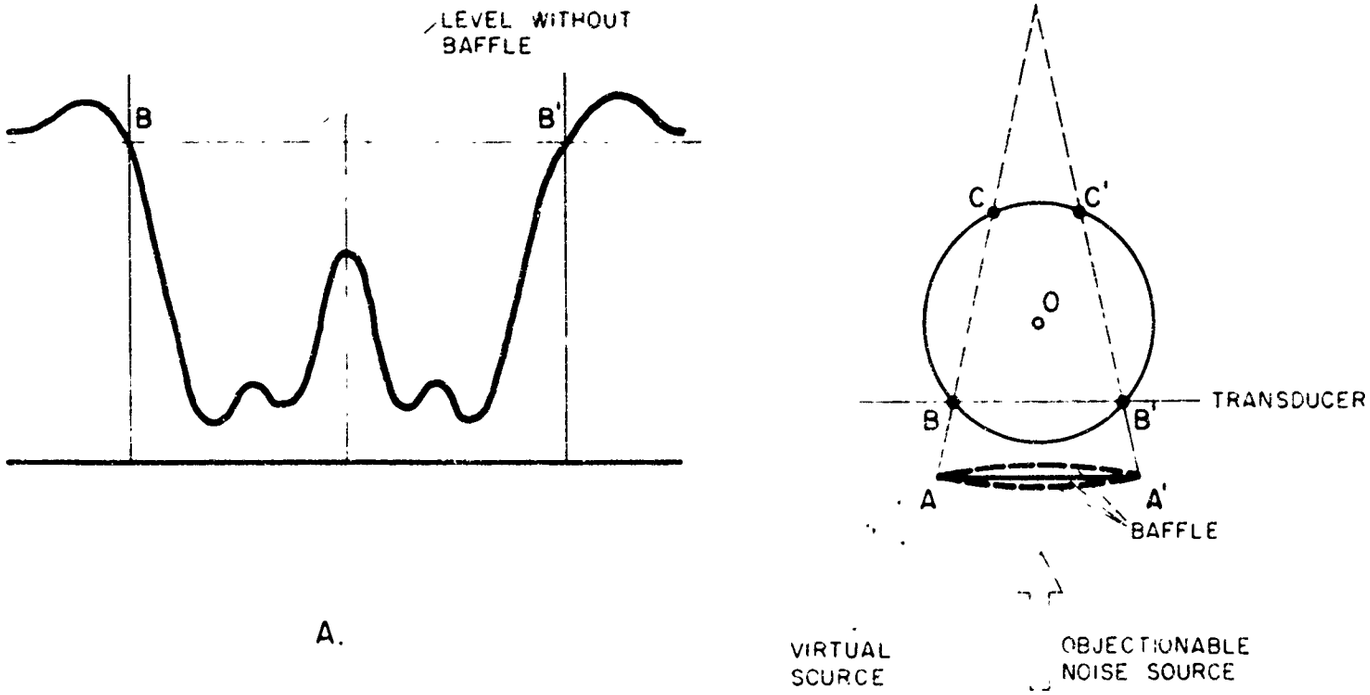

Fig. 6- SCHEMATIC REPRESENTATION OF A COMPOSITE DIFFRACTION PATTERN AND ITS RELATION TO THE BAFFLE-TRANSDUCER SYSTEM

that the sound field in the regions BC and B'C' will be spatially coherent, and the exact phase relationships, as they exist in the modified sound field, will cause this coherent sound field to appear to originate from a source located (in azimuth) in the vicinity of the baffle edges (the virtual source in Figure 6b). Because this noise field is coherent, it will be summed in the beam forming process, like a coherent signal, modified only by the beam pattern in the direction of the virtual source. For example, a beam which is designed to "look" in the direction OC will have a finite response in the direction of the virtual source. Situations are not uncommon in which this virtual source can be some 20 db or more greater than the ambient noise level in the pass band of interest. If the beam is not shaded or compensated, it is not unlikely that for a number of beam positions the virtual source may be received on a side lobe no more than 12 to 15 db down from the major lobe. If a sufficient number, say about half, of the elements used to form a beam are in the region of high intensity, the total noise output from the beam can be significantly greater than for sea or water flow noise alone. This coherent noise output is interpreted by the equipment as a signal on the major lobe axis. Because this coherent noise signal is continuous, it will appear, in an active sonar, at all ranges, i.e., produce a "spoke" on a PPI presentation. Note that such spokes can appear both fore and aft.

The production of these false signals by the interaction between the noise field behind the baffle (primarily the diffraction pattern) and the beam pattern will occur whether the baffle is large enough to place the transducer completely in a region of lower intensity than ambient or not because the field is not constant across the diffraction shadow. Within the shadow, however, this interaction will occur to a much lesser degree.

It is interesting to note that the interaction between the virtual noise source and the beam pattern can be minimized by the

use of shading (except, of course, in the direction of the source). Stated more generally, baffle design and beam forming (either for fixed beams or for the rotating beams) cannot be carried out independently unless shading is used to a degree that the side lobes are down far enough to make the virtual source negligible.

From the point of view of baffle design, it appears that the diffraction characteristics of a baffle require further study and analysis than do the transmission characteristics.

As pointed out above noise transmission through the baffle has been reduced largely to a development or selection of materials. Until the diffraction effects can be delineated, the value of further baffle material development is not known, because there is, after all no reason to reduce the noise transmitted through the baffle much below the level of the diffracted noise field. This may be possible now with available materials.

APPENDIX 1

1.1 Diffraction Around a Baffle-Normal Incidence

The appendix will analyze the diffraction of sound around an infinite strip baffle. The baffle is of width 2a, and composed of pressure release or absorbing surface, i.e., the particle velocity is zero on the baffle surfaces. The general non-viscous wave equation is used to describe the sound field. The boundary condition of an undistorted plane wave in the plane of the baffle is used to describe the incident sound. The baffle is referred to the coordinate system shown in Figure A1.1.1.

A plane wave propagating in the positive y direction can be represented by

$$\psi_I = \psi_o e^{-(i\omega t - ikx)} , \tag{1}$$

where ψ_I = scalar velocity potential of the incident wave
ω = frequency of the sound wave
k = wave number ($k = \frac{2\pi}{\lambda}$, λ = wave length).

To determine the solution to the problem, first consider the general wave equation

$$\nabla^2 \psi = \frac{1}{c^2} \frac{\partial^2 \psi}{\partial t^2} \tag{2}$$

where c is the propagation velocity in the medium (velocity of sound). Two important properties of velocity potential function are given by

$$\frac{\partial \psi}{\partial n} = v_n \tag{3}$$

$$\frac{\partial \psi}{\partial t} = - \frac{p}{\rho} \tag{4}$$

where v_n is the particle velocity in the n-direction, ρ is the

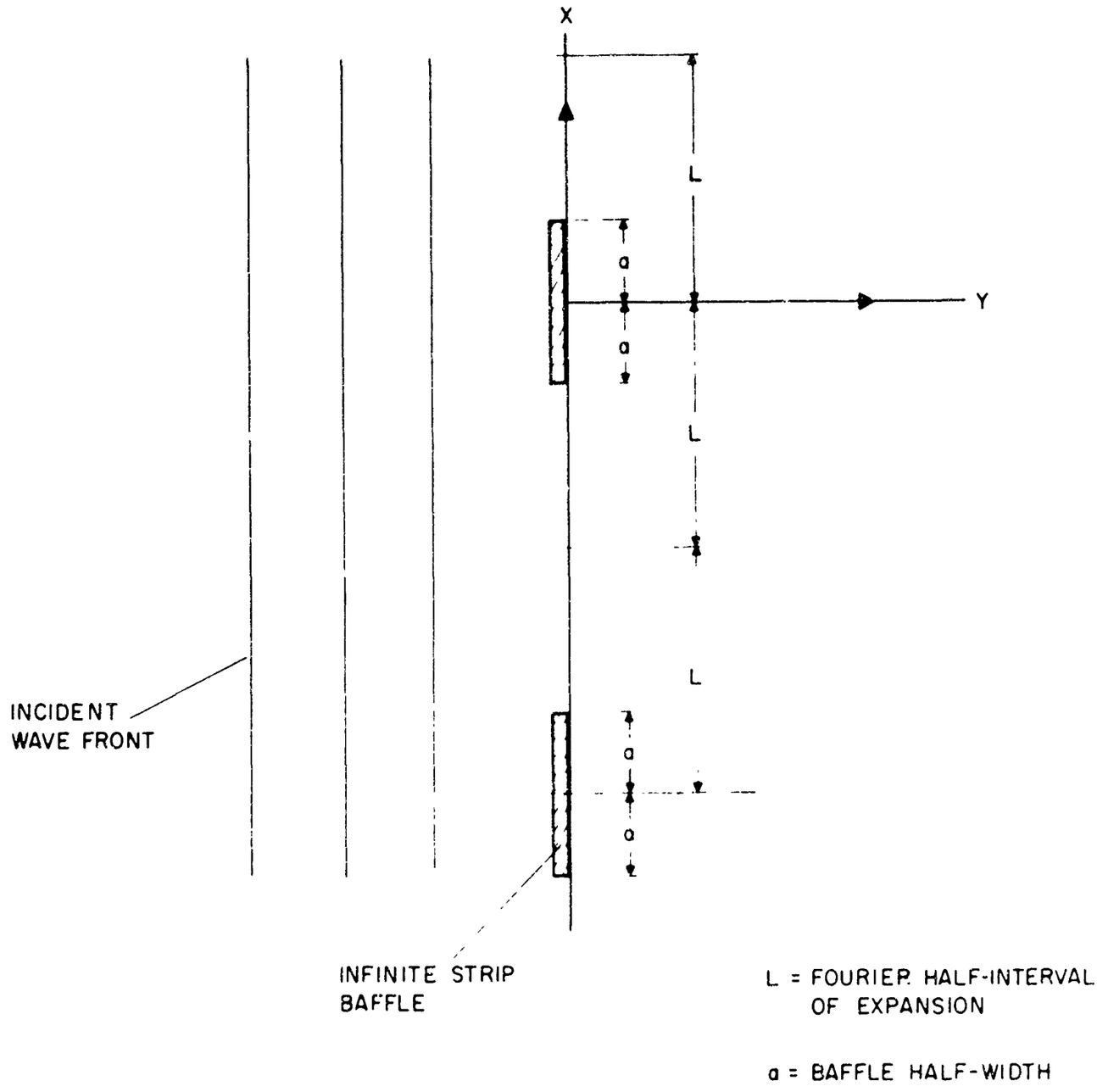

Fig. A1.1.1 – COORDINATE SYSTEM FOR THE DIFFRACTION AROUND AN INFINITE STRIP BAFFLE FOR A NORMALLY-INCIDENT PLANE WAVE

density of the medium, and p is the instantaneous sound pressure. These two properties will be used later in the determination of boundary conditions. By considering an infinite baffle, the problem is reduced to two dimensions. Thus Equation (2) in cartesian coordinates become

$$\frac{\partial^2 \psi}{\partial x^2} + \frac{\partial^2 \psi}{\partial y^2} = \frac{1}{c^2} \frac{\partial^2 \psi}{\partial t^2} \, . \tag{5}$$

The general form of the solution to Equation (4) is taken to be

$$\psi = X(x)Y(y)e^{-i\omega t} \tag{6}$$

where X(x), Y(y) are continuous, analytic functions of x and y. Using this solution, Equation (6) in the governing Equation (5), yields the equations,

$$\frac{d^2X}{dx^2} + \ell^2 X = 0 \tag{7}$$

$$\frac{d^2Y}{dy^2} + m^2 Y = 0 \tag{8}$$

$$\ell^2 m^2 = \omega^2/c^2 \tag{9}$$

where ℓ and m are separation constants. A solution of Equations (7), (8), and (9) is

$$\left.\begin{aligned} X &= A + Bx \\ Y &= A' + B'y \end{aligned}\right\} \; h, \ell = 0 \tag{10}$$

$$\left.\begin{aligned} X &= C \sin \ell_n x + D \cos \ell_n x \\ Y &= C' \sin h_n y + D' \cos h_n y \end{aligned}\right\} \quad h_n, \ell_n \neq 0 \tag{11}$$

where

$$h_n = \left[\omega^2/c^2 - \ell_n^2\right]^{1/2} \quad . \tag{12}$$

Since Equation (6) is a linear equation and ℓ is any real constant, a linear combination of the solutions (10) and (11) is also a solution. Therefore, the general solution can be written in the form

$$\psi = \sum_n (A_n \sin \ell_n x + B_n \cos \ell_n x)(C_n \sin h_n y + D_n \cos h_n y)\, e^{-i\omega t}$$
$$h_n = \left[\omega^2/c^2 - \ell_n^2\right]^{1/2} \tag{13}$$

where A_n, B_n, C_n, D_n are arbitrary constants. These constants will be evaluated from the boundary conditions. Since the baffle is assumed to be a pressure release surface, the incident wave reaches the plane ($y = 0$) undistorted and the particle velocity is zero on the strip baffle. For the case of the normally incident wave, i.e., wave fronts parallel to the surface of the baffle, the boundary surface becomes an infinite piston with a strip the size of the baffle held fixed. The condition on the surface of the baffle, recalling Equation (3), becomes

$$\left.\frac{\partial \psi}{\partial y}\right|_{y=0} = 0 \qquad \text{for} \qquad 0 \leq |x| \leq a \tag{14}$$

and

$$\left.\frac{\partial \psi}{\partial y}\right|_{y=0} = v_{yI} \qquad \text{for} \qquad |x| > a \tag{15}$$

where v_{yI} is the particle velocity in the incident plane wave. These conditions, plus the requirement that at large distances from the baffle the solution becomes plane waves again, determine the solution.

Equations (14) and (15) can be rewritten in the form

$$\frac{\partial \psi}{\partial y} = v_{yI}\, S_a(x) \ , \tag{16}$$

where $S_a(x)$ is the unit step function in the interval $a < x < \infty$. From Equations (1) and (2) the particle velocity in the incident wave is

$$v_{yI.} = \frac{\partial \psi_I}{\partial y} = ik\psi_o e^{-i(\omega t - kx)} \tag{17}$$

Expanding Equation (16) in a Fourier series in the interval 2L, where $L >> a$, and combining with Equation (17) yields,

$$v_y = \psi_o ik \left\{(1 - a/L) - \sum_{j=1}^{\infty} \frac{2}{j\pi} \sin \frac{j\pi a}{L} \cos \frac{j\pi x}{L}\right\} e^{-i\omega t} \ . \tag{18}$$

From Equation (13) the particle velocity in the plane of the baffle is

$$v_y = \sum_n h_n \left[A_n \sin \ell_n x + B_n \cos \ell_n x\right] C_n e^{-i\omega t} \ . \tag{19}$$

The boundary conditions given by Equations (18) and (19) must be term wise identical. This condition yields

$$\begin{aligned} A_n &\equiv 0 && \text{(a)} \\ \ell_n &= \frac{j\pi}{L} && \text{(b)} \end{aligned} \tag{20}$$

$$C_o B_o = \frac{\psi_o}{2}\left[1 - a/L\right] \qquad (c)$$

$$C_n B_n = -\psi_o \frac{\sin \frac{j\pi a}{L}}{j\pi\sqrt{1 - \left(\frac{j\lambda}{2L}\right)^2}} \cdot \qquad (d) \qquad (20)$$

Using Equation (20) in Equation (13) gives

$$\psi = \psi_o e^{-i\omega t}\left\{(1 - a/L)\sin\frac{\omega}{c}y - \sum_{n=1}^{\infty}\frac{2\sin\frac{n\pi a}{L}}{n\pi\sqrt{1-\gamma_n^2}}\cos\frac{n\pi x}{L}\sin\sqrt{1-\gamma_n^2}\,y + \sum_n B_n D_n \cos\frac{n\pi x}{L}\cos\sqrt{1-\gamma_n^2}\,y\right\}, \qquad (21)$$

where $\gamma_n = \frac{n\lambda}{2L}$. Notice in Equation (21) that the radical in the argument of the y function becomes imaginary for values of γ_n $n > N$. For the solution to remain finite under such conditions $B_n D_n$ must be identically zero. Writing the solution, Equation (21), with the y-terms in exponential form yields

$$\psi = \psi_o e^{-i\omega t}\left\{(1 - a/L)e^{i\frac{\omega}{c}y} - \sum_{n=1}^{\infty}\frac{2\sin\frac{n\pi a}{L}}{n\pi\sqrt{1-\gamma_n^2}}\cos\frac{n\pi x}{L}\,e^{i\sqrt{1-\gamma_n^2}\,y}\right\}. \qquad (22)$$

Note that the solution changes form for $n > N$. This change is best noted by rewriting the solution in the form

$$\psi = \psi_o e^{-i\omega t}\left\{(1 - a/L)e^{i\frac{\omega}{c}y} - \sum_{n=1}^{N}\frac{2\sin\frac{n\pi a}{L}}{n\pi\sqrt{1-\gamma_n^2}}\cos\frac{n\pi x}{L}\,e^{i\sqrt{1-\gamma^2}} + \sum_{n=N+1}^{\infty} i\frac{2\sin\frac{n\pi a}{L}}{n\pi\sqrt{\gamma_n^2 - 1}}\cos\frac{n\pi x}{L}\,e^{-\sqrt{\gamma_n^2-1}\,y}\right\} \qquad (23)$$

for $N > \frac{2L}{\lambda} > N + 1$. Equation (23) can be written in the form

$$\frac{\psi}{\psi_o} = A(x,y)\, e^{-i\left[\omega t - \theta(x,y)\right]} \tag{24}$$

where

$$A^2(x,y) = \left[(1 - \frac{a}{L}) \sin \frac{\omega}{c} y - \sum_{1}^{N} \frac{2 \sin \frac{n\pi a}{L}}{n\pi \sqrt{1 - \gamma_n^2}} \cos \frac{n\pi x}{L} \sin \sqrt{1 - \gamma_n^2}\, y \right]^2$$

$$+ \left[(1 - \frac{a}{L}) \cos \frac{\omega}{c} y - \sum_{1}^{N} \frac{2 \sin \frac{n\pi a}{L}}{n\pi \sqrt{1 - \gamma_n^2}} \cos \frac{n\pi x}{L} \cos \sqrt{1 - \gamma_n^2}\, y \right. \tag{25}$$

$$\left. + \sum_{N+1}^{\infty} \frac{2 \sin \frac{n\pi a}{L}}{n\pi \sqrt{\gamma_n^2 - 1}} \cos \frac{n\pi x}{L}\, e^{-\sqrt{\gamma_n^2 - 1}\, y} \right]^2$$

and

$$\theta = \mathrm{Tan}^{-1} \frac{R_e}{I_m} \quad . \tag{26}$$

R_e is the first bracketed term of Equation (25) and I_m is the second bracketed term of Equation (25). Equation (25) gives the amplitude ratio of the potential functions which, from Equation (4) is also the pressure amplitude ratio.

Equation (25) was programmed for a digital computer, and the ratio, A(x,y) was calculated for various values of the non-dimension ratios, $\frac{a}{\lambda}$, $\frac{a}{L}$, and $\frac{\omega}{c}$ y. Results from these calculations are shown in Figures 2 and 3 in Section 2.

To extend the solution to a source of finite bandwidth Equation (24) can be integrated over this bandwidth. However, Equation (24) does not readily yield to analytic integration over a frequency band.

But, as has been indicated above, Equation (24) can be readily programmed for solution by a digital computer and, since ψ is a linear function, a numerical integration is admissible. The finite bandwidth can be subdivided into elemental bands. The energy in the elemental band is assigned to the center frequency of this band. A summation over the center frequencies can be carried out by the digital computer and results for the finite bandwidth source can be evaluated.

1.2 Diffraction Around a Baffle-Oblique Incidence

The development of a solution for a wave obliquely incident on the infinite strip baffle parallels that for the normal-incidence case. Only the salient features of the oblique case will be demonstrated here.

The coordinate system used is shown in Figure A.1.2.1.

It is assumed that a freely-progressive plane wave described by

$$\Psi_o = \Psi_o e^{-i(\omega t - k_x x - k_y y)} \tag{1}$$

where

Ψ = scalar velocity potential,

ω = angular frequency of wave,

k_x = projected wave number in x direction,

k_y = projected wave number in y direction,

is obliquely incident on a rigid semi-infinite strip of negligible thickness lying in the plane y = 0. The strip is infinite in extent perpendicular to the x - y plane. That the strip is rigid implies that the particle velocity normal to the strip is zero in the region $-a \leq x \leq a$.

The variables of the wave equation are separable in the manner shown in the normal-incidence solution. Upon separation of variables and solution of the resulting ordinary differential equations one may determine a general solution of the form

$$\Psi = \sum_j \left(A_j e^{\sqrt{k_j^2}\, x} + B_j e^{-\sqrt{k_j^2}\, x} \right) \left(C_j e^{i\sqrt{k^2 + k_j^2}\, y} + D_j e^{-i\sqrt{k^2 + k_j^2}\, y} \right) e^{-i\omega t} \tag{2}$$

where

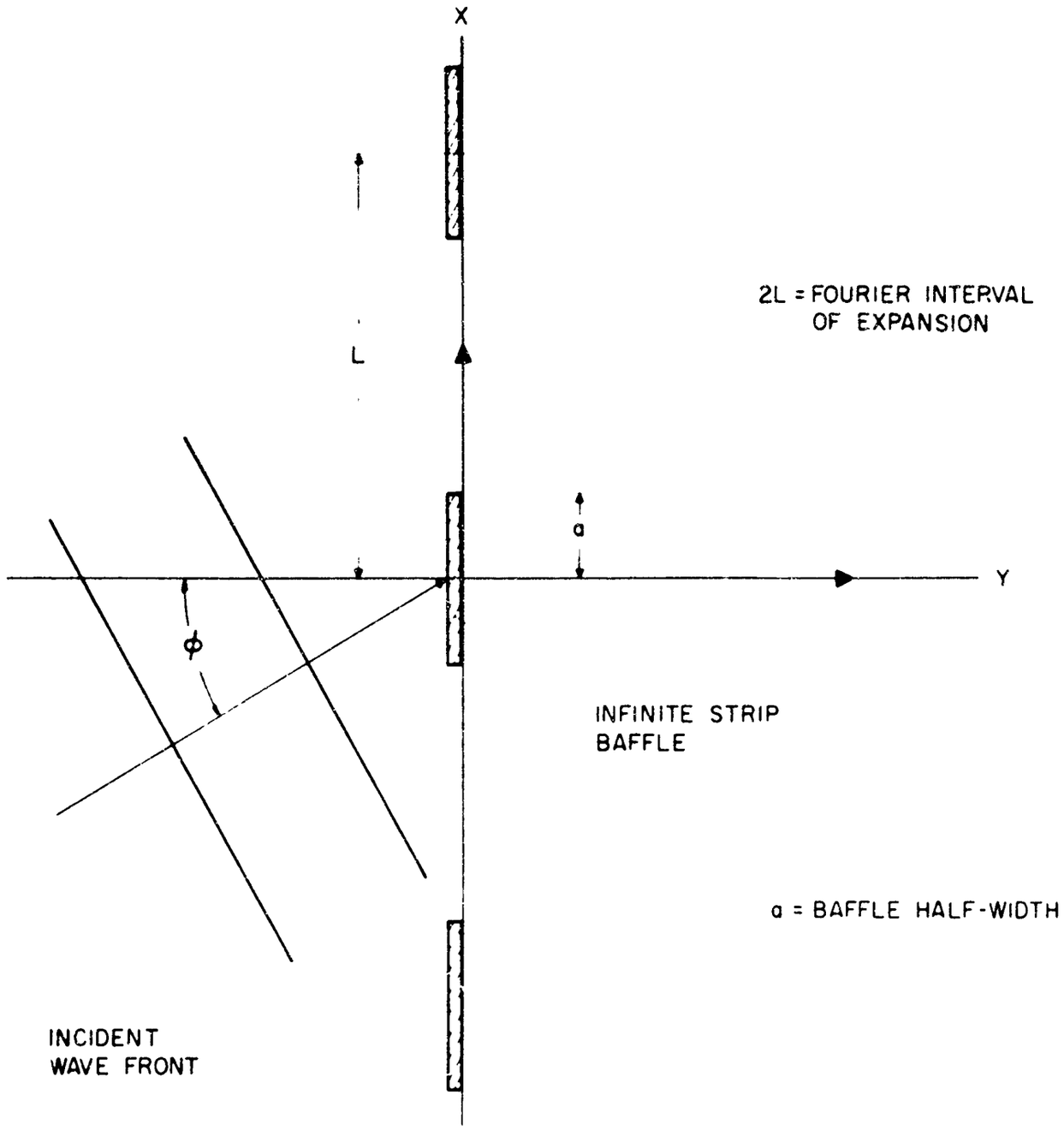

Fig. A1.2.1 – COORDINATE SYSTEM FOR THE DIFFRACTION AROUND AN INFINITE STRIP BAFFLE OF AN OBLIQUELY-INCIDENT PLANE WAVE

A_j, B_j, C_j, D_j = undetermined coefficients, perhaps complex in form;

k_j = an undetermined separation constant, either real or imaginary;

and k = wave number ω/C.

In determining a boundary condition, the point of view of an observer sitting in the $y = 0$ plane will be taken. Such an observer sees a plane wave approach the strip at an angle ϕ. In general the particle velocity of the wave in the y direction is

$$v_y = \frac{\partial \psi}{\partial y} = ik_y \psi_o e^{-i(\omega t - k_x x - k_y y)}. \tag{3}$$

At the plane $y = 0$, however, the particle velocity in the y direction is reduced to zero in the region $-a \leq x \leq a$ because the strip is rigid. Hence,

$$\left.\frac{\partial \psi}{\partial y}\right|_{y=0} = ik_y \psi_o e^{-i(\omega t - k_x x)} S_a(x) \tag{4}$$

where

$2a$ = width of strip and $S_a(x)$ is the unit step function $S_a(x) = 0$, $0 \leq x < a$, and $S_a(x) = 1$, $a \leq x < \infty$.

For the assumed solution (2) to be valid, it must fit the boundary condition (4).

The boundary condition (4) may be expressed in a Fourier series. Equation (4) can be written in the form

$$\left.\frac{\partial \psi}{\partial y}\right|_{y=0} = ik_y \psi_o (\cos k_x x + i \sin k_x x) S_a(x) e^{-i\omega t}. \tag{5}$$

The general form of the Fourier expansion is

$$\left.\frac{\partial \psi}{\partial y}\right|_{y=0} = \frac{a_o}{2} + \sum_{n=1}^{\infty} \left(a_n \cos \frac{n\pi x}{L} + b_n \sin \frac{n\pi x}{L}\right), \tag{6}$$

where L is an arbitrary interval of expansion.

The Fourier coefficients for the expansion of (5) are determined in the usual manner, resulting in the following Fourier series expansion of the boundary condition.

$$\left.\frac{\partial \psi}{\partial y}\right|_{y=0} = \left\{\frac{1}{2} ik_y \psi_o M_o + \sum_{n=1}^{\infty} \left(ik_y \psi_o M_n \cos \frac{n\pi x}{L} - k_y \psi_o N_n \sin \frac{n\pi x}{L}\right)\right\} e^{-i\omega t} \tag{7}$$

where

$$M_o = 2 \frac{(\sin k_x L - \sin k_x a)}{k_x L}, \tag{8}$$

$$M_n = 2\left\{\frac{k_x L \left[(-1)^n \sin k_x L - \sin k_x a \cos \frac{n\pi a}{L}\right] + n\pi \cos k_x a \sin \frac{n\pi a}{L}}{k_x^2 L^2 - n^2 \pi^2}\right\} \tag{9}$$

and

$$N_n = 2\left\{\frac{n\pi \left[(-1)^n \sin k_x L - \sin k_x a \cos \frac{n\pi a}{L}\right] + k_x L \cos k_x a \sin \frac{n\pi a}{L}}{k_x^2 L^2 - n^2 \pi^2}\right\}. \tag{10}$$

Using the assumed solution (2), $\left.V_y\right|_{y=0}$ is given by

$$\left.\frac{\partial \psi}{\partial y}\right|_{y=0} = \sum_{j=1}^{\infty} \left(A_j e^{\sqrt{k_j^2}\, x} + B_j e^{-\sqrt{k_j^2}\, x}\right)\left(i\sqrt{k^2 + k_j^2}\right)\left(C_j - D_j\right) e^{-i\omega t}. \tag{11}$$

For the assumed solution (2) to fit the boundary condition (4), Equations (7) and (11) must be equated term by term. It can be seen that for such a relation to exist,

$$k_j = i \frac{n\pi}{L} . \tag{12}$$

The only restriction on the solution (2), other than the boundary condition (4) is that it remain finite for all positive y. This restriction, together with the relation (12), can be used to eliminate D_j. Consider the term

$$D_j e^{-i\sqrt{k^2 + k_j^2}\, y} .$$

For large n this term becomes

$$D_j e^{\sqrt{\frac{n^2\pi^2}{L^2} - k^2}\, y}$$

which does not lead to a bounded solution. Hence D_j must be identically zero. Equation (12) can now be rewritten as

$$\left.\frac{\partial \psi}{\partial y}\right|_{y=0} = \sum_{n=1}^{\infty} \left[A_n(\cos \frac{n\pi x}{L} + i \sin \frac{n\pi x}{L}) + B_n (\cos \frac{n\pi x}{L} - i \sin \frac{n\pi x}{L})\right]$$

$$i \left(k^2 - \frac{n^2\pi^2}{L^2}\right) e^{-i\omega t} . \tag{13}$$

Equating cosine and sine components from Equations (7) and (13) results in

$$i\alpha_n (A_n + B_n) = i k_y \psi_o M_n , \tag{14}$$

and

$$\alpha_n (- A_n + B_n) = - k_y \psi_o N_n .$$

Here

$$\alpha_n = \sqrt{k^2 - \frac{n^2\pi^2}{L^2}} .$$

Solving Equations (14) for A_n and B_n yields

$$A_n = \frac{k_y \psi_o}{2\alpha_n} (M_n + N_n) \quad (1$$

and

$$B_n = \frac{k_y \psi_o}{2\alpha_n} (M_n - N_n) . \quad (1$$

The form of the solution now becomes

$$\frac{\psi}{\psi_o} = \left\{ \frac{k_y}{2\alpha_o} M_o e^{i\alpha_o y} + \sum_{n=1}^{\infty} \left[\frac{k_y}{2\alpha_n} (M_n + N_n)\left(\cos \frac{n\pi x}{L} + i \sin \frac{n\pi x}{L}\right) \right.\right.$$

$$\left.\left. + \frac{k_y}{2\alpha_n} (M_n - N_n)\left(\cos \frac{n\pi x}{L} - i \sin \frac{n\pi x}{L}\right) \right] e^{i\alpha_n y} \right\} e^{-i\omega t} . \quad (1$$

It is convenient to modify Equation (17) in order to obtain a form suitable for computations.

$$\alpha_n = \sqrt{k^2 - \frac{n^2\pi^2}{L^2}} . \quad (1$$

Note that for $n > N$ $\left(N = \frac{k_y L}{\pi}\right)$, $\alpha_n = i\,\beta_n$, where

$$\beta_n = \sqrt{\frac{n^2\pi^2}{L^2} - k^2} . \quad (1$$

It is therefore convenient to break the infinite series (17) into two series having summation ranges of $1 \leq n \leq N$, and $N + 1 \leq n < \infty$. Further, let

$$\gamma = \frac{n\lambda}{2L} , \quad (2$$

where λ is the wave length of the incident wave. α_n and β_n become

$$\alpha_n = k\sqrt{1 - \gamma^2} \tag{21}$$

and

$$\beta_n = k\sqrt{\gamma^2 - 1} \ , \tag{22}$$

where k is the wave number of the incident wave.

With these modifications, retaining only the real parts of Equation (17), the solution can be written in the form

$$\frac{\psi}{\psi_o} = \left(\frac{\psi}{\psi_o}\right)_c \cos \omega t + \left(\frac{\psi}{\psi_o}\right)_s \sin \omega t \ . \tag{23}$$

The coefficients $\left(\frac{\psi}{\psi_o}\right)_c$ and $\left(\frac{\psi}{\psi_o}\right)_s$ are after some simplification,

$$\left(\frac{\psi}{\psi_o}\right)_c = \frac{1}{2} M_o \cos \alpha_o y + \sum_{n=1}^{N} \frac{k \cos \phi}{\alpha_n} \left(M_n \cos \frac{n\pi x}{L} \cos \alpha_n y \right.$$

$$\left. - N_n \sin \frac{n\pi x}{L} \sin \alpha_n y\right) + \sum_{n=N+1}^{\infty} \frac{k \cos \phi}{\beta_n} N_n \sin \frac{n\pi x}{L} \ e^{-\beta_n y} \tag{24}$$

and

$$\left(\frac{\psi}{\psi_o}\right)_s = \frac{1}{2} M_o \sin \alpha_o y + \sum_{n=1}^{N} \frac{k \cos \phi}{\alpha_n} \left(M_n \cos \frac{n\pi x}{L} \sin \alpha_n y \right.$$

$$\left. + N_n \sin \frac{n\pi x}{L} \cos \alpha_n y\right) - \sum_{n=N+1}^{\infty} \frac{k \cos \phi}{\beta_n} M_n \cos \frac{n\pi x}{L} \ e^{-\beta_n y} \ , \tag{25}$$

where

$$\alpha_n = k\sqrt{1 - \gamma^2}$$

$$\beta_n = k\sqrt{\gamma^2 - 1} .$$

A solution for the special case of zero angle of incidence ($\phi = 0$) has been obtained independently and is given in Appendix 1.1. The solution for a general angle of incidence can be reduced to the normal-incidence solution by the substitution of $\phi = 0$ in the above Equations (24) and (25).

A particular solution is demonstrated in Figure 3. The parameters used in this solution were;

$$\phi = 20^{\circ}$$

$$\lambda = .5 \text{ ft}$$

$$a = 4\lambda$$

$$L = 40\lambda .$$

The intensity of the diffracted wave normalized to the incident-wave intensity at intervals $\Delta y = 2\lambda$ beginning at the plane of the strip are shown in the figure.

A complete analysis of the baffle considered alone requires the construction of a solution for a complex sound field, that is, a field having waves of arbitrary equiphase lines and a continuous frequency distribution.

An effort to obtain an integral of Equation (23) using a continuously distributed semi-circular source indicated that a spatially distributed source can most conveniently be treated numerically. The technique considered is illustrated as follows:

assume a single frequency arc-shaped source at some distance from and symmetric with respect to the baffle. The source can be approximated, to the first order, by two in-phase equal-amplitude plane waves as shown in Figure A1.1.2. Of course, the use of several in-phase plane waves effects a more accurate representation of the source. For more complex sources, it is not expected that the phase or amplitude relation will be so simple; however, such sources can be approximated by a superposition of plane waves having appropriate angles of incidence with respect to the baffle.

It was pointed out in the previous section that frequency distributions can be approximated by a summation over intervals of the frequency band. Combining the spatial and frequency summations, the solution to a complex field will have the general form

$$\psi = \sum_{m} \sum_{n} f_{n,m} \psi_o e^{-i(\omega_m t - k_{x_{n,m}} x - k_{y_{n,m}} y)}$$

where $f_{n,m}$ is an amplitude and frequency weighting function.

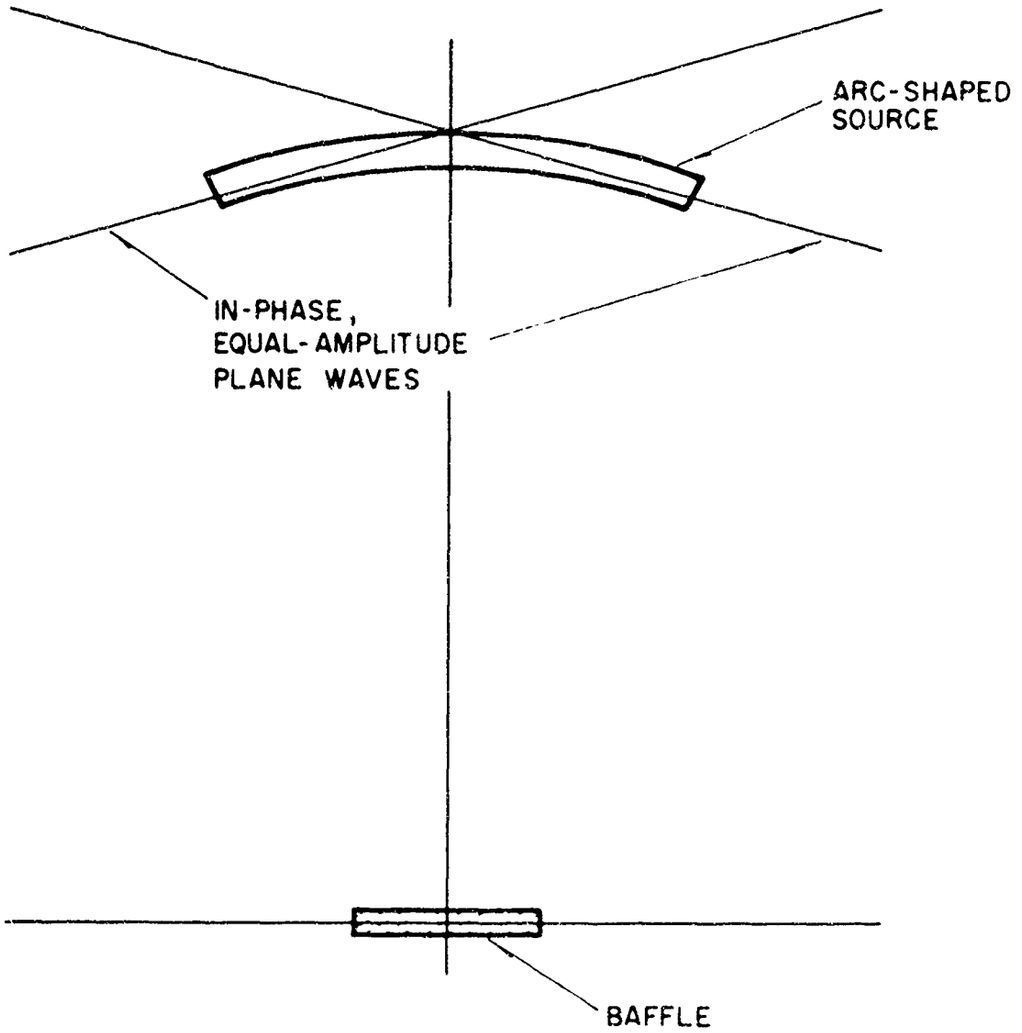

Fig. A1.2.2 - PLANE WAVE APPROXIMATION TO A CONTINUOSLY-DISTRIBUTED ARC-SHAPED SOURCE BY TWO IN-PHASE, EQUAL-AMPLITUDE PLANE WAVES

APPENDIX 2

2.1 The Transmission of Sound Through Sonar Domes

The theory treating transmission and attenuation of sound in flat plates is highly developed in the literature.* Baffles encountered in sonar applications are readily approximated by attenuating flat layers and can be analyzed using flat plate results.[1] Hence the baffle study was reduced to that of materials selection and is discussed in Section 2.2 below.

The problem to be considered here is to determine the effect of the sonar dome on the incident sound. Transmission theory treating complex plate shapes is not well developed and exists only for shapes such as hemispherical[2] and cylindrical shells. No previous work was found which treated irregular shapes. Therefore the sonar dome shape has been treated by approximating it with a series of flat plates. The dome transmittivity is described using flat plate data. To introduce this technique, a discussion of flat plate transmittivity follows.

Consider the situation pictured in Figure A2.1.1. The incident wave front represents a plane harmonic wave impinging on a segment of a dome or baffle at a general angle of incidence. Part of the incident energy is reflected and the balance is transmitted through the layer. The objective of the study is to develop an expression for the transmission coefficient, T, which is a complex quantity whose modulus represents the ratio of transmitted-to-incident pressure and the phase is the phase shift occurring in transmission.

Standard boundary conditions are applied at liquid-solid interfaces, governing the passage of sound energy from one medium to the next. These conditions are: the liquid surrounding the baffle supports only longitudinal (compressional) waves; there exists a

---

*See listed References.

[1]See, for example, Reference 3.

[2]See Reference 8.

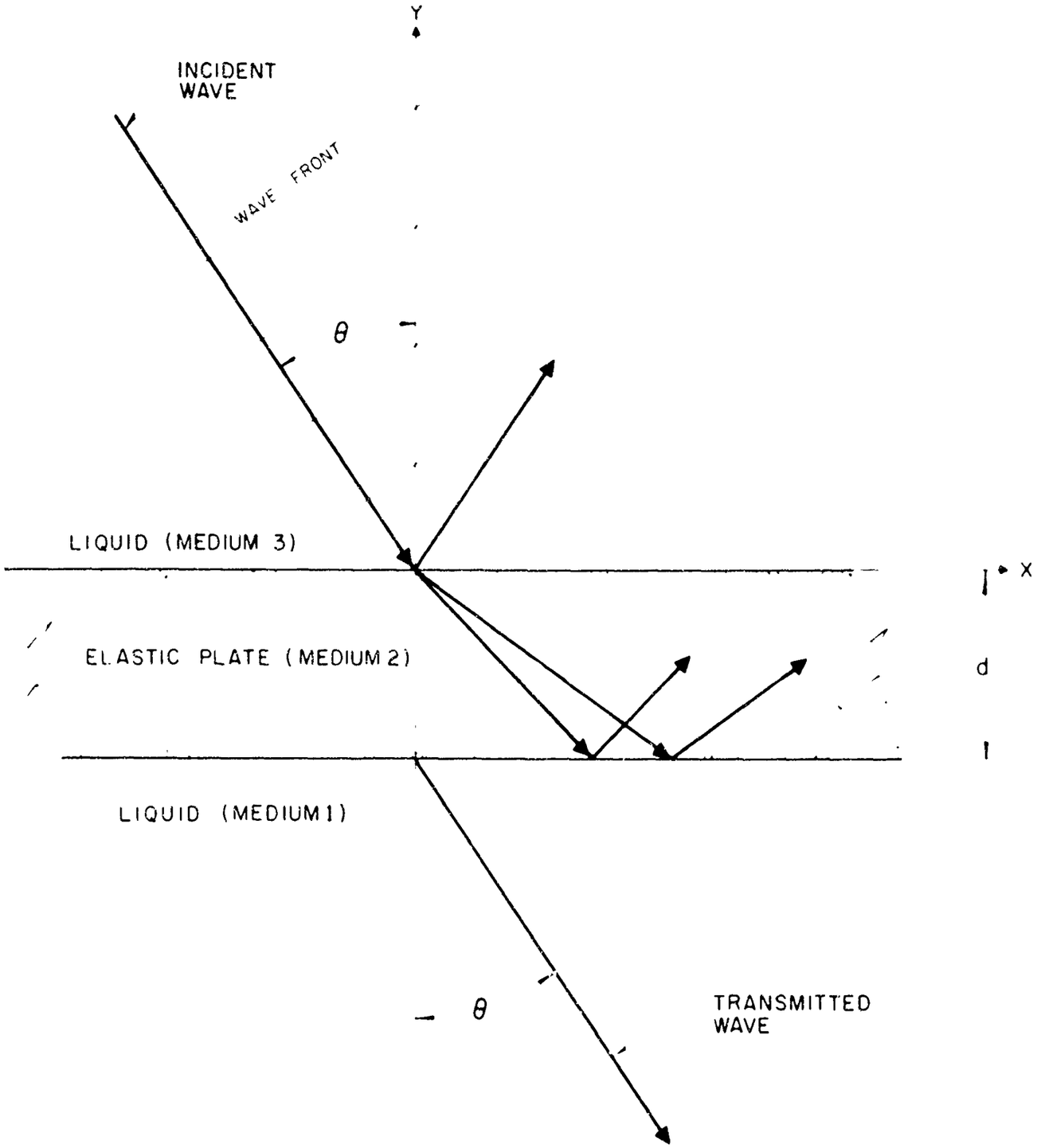

Fig. A2.1.1 – TRANSMISSION OF A PLANE SOUND WAVE THROUGH AN ELASTIC PLATE

TEXAS RESEARCH ASSOCIATES
AUSTIN, TEXAS 9-25-61
DWG 2000-21 FG JRR

continuity of normal stresses and normal displacements across the boundary. The tangential stress components must be continuous across the interface, but since the water does not support shear stress, this condition reduces to the condition that the tangential stress vanishes at the interface. The solution satisfying the sound field in the system is assumed to be plane harmonic waves of a single frequency.

The incident plane wave impinges on a layer of finite thickness d, at an arbitrary angle of incidence, θ (refer to Figure A2.1.1). The subscripts 1, 2, and 3 denote respectively the medium into which transmission occurs, the baffle medium, and the medium of the incident wave.

The pressure amplitudes can be related through the use of normal acoustic impedances, which are defined as the ratio of acoustic pressure to the normal particle velocity. Normal acoustic impedance can be written for a medium as

$$Z = \frac{\rho c}{\cos \vartheta} \qquad (1)$$

Since this quantity is composed of pressure (or normal stress) and normal velocity (related to normal particle displacement), and each of these elements are continuous across boundaries of media, the normal acoustic impedance must be continuous across boundaries of the media.

Considering first the impedance of a single layer baffle (medium 2); the acoustic pressure wave transmitted into the baffle can be written

$$p_2 = \left[A\, e^{-i\alpha_2 y} + B\, e^{i\alpha_2 y} \right] e^{i(\sigma_2 x - \omega t)}, \qquad (2)$$

where $\alpha = k \cos \theta$, $\sigma = k \sin \theta$. Here k is the wave number $\frac{\omega}{c}$ and A and B are undetermined amplitude coefficients. The normal component of particle velocity can be written

$$v_2 = \frac{1}{Z_2}\left[A\, e^{-i\alpha_2 y} + B\, e^{i\alpha_2 y}\right] e^{i(\quad x - \omega t)} \quad . \tag{3}$$

Now the characteristic impedance for medium 2 can be formed as the ratio $Z_2 = p_2/v_2$. At the 1-2 boundary, Z_2 must equal Z_1; i.e., for $y = 0$,

$$Z_2 \frac{A + B}{A - B} = Z_1 \quad \text{or} \quad \frac{B}{A} = \frac{Z_1 - Z_2}{Z_1 + Z_2} \quad . \tag{4}$$

This same reasoning of "continuity of impedances" at the upper boundary 2-3 (where $y = d$) gives

$$Z_2 = \frac{A\, e^{-i\alpha_2 d} + B\, e^{i\alpha_2 d}}{A\, e^{-i\alpha_2 d} - B\, e^{i\alpha_2 d}} \quad . \tag{5}$$

Substitution for $\frac{B}{A}$ from Equation (4) into Equation (5) gives

$$Z_{in} = \frac{Z_1 - iZ_2 \tan \alpha_2 d}{Z_2 - iZ_1 \tan \alpha_2 d} Z_2 . \tag{6}$$

Equation (6) is an expression for the input impedance to the layer in terms of the characteristic impedances of media 1 and 2 and the layer thickness.

Introducing the elements of the acoustic impedance of medium 3 and applying the condition of "impedance continuity" across the boundary $y = d$ gives with the factor $e^{i\omega t}$ suppressed,

$$p_3 = \left[C\, e^{-i\alpha_3 (y - d)} + D\, e^{i\alpha_3 (y - d)}\right] e^{i \quad x} \tag{7}$$

and

$$v_3 = \frac{1}{Z_3}\left[C\, e^{-i\alpha_3(y - d)} - D\, e^{i\alpha_3(y - d)}\right] e^{i\sigma_3 x} \quad . \tag{8}$$

At the interface $y = d$, the ratio $\frac{p_3}{v_3}$ must represent the input impedance Z_{in} of the layer, i.e.,

$$Z_{in} = Z_3 \frac{C + D}{C - D} \quad . \tag{9}$$

In Equations (7) and (8), the pressure and velocity in medium 3, C denotes the amplitude of an incident pressure wave and D is the amplitude of a reflected wave. The ratio D/C is the reflection coefficient V, and is used in the formulation of the transmission coefficient T. From Equation (9) the reflection coefficient can be written

$$V = \frac{D}{C} = \frac{Z_{in} - Z_3}{Z_{in} + Z_3} \quad , \tag{10}$$

where Z_{in} is given by Equation (6). Substituting Equation (6) into Equation (10) gives

$$V = \frac{(Z_1 + Z_2)(Z_2 - Z_3)\, e^{-i\alpha_2 d} + (Z_1 - Z_2)(Z_2 + Z_3)\, e^{i\alpha_2 d}}{(Z_1 + Z_2)(Z_2 + Z_3)\, e^{-i\alpha_2 d} + (Z_1 - Z_2)(Z_2 - Z_3)\, e^{i\alpha_2 d}} \quad . \tag{11}$$

The sound field in medium 1 is the energy transmitted through the baffle. It can be expressed by

$$p_1 = G\, e^{-i\,(\alpha_1 y - \sigma_i x)} \quad , \tag{12}$$

where G is the amplitude of the transmitted pressure wave. The transmission coefficient T according to the definition is $T = G/C$.

Applying the condition of continuity of normal stress or sound pressure at the interfaces, T can be formulated in terms of the known quantities. At the 1-2 interface, where y = 0, the pressure expressions Equations (2) and (12) have the same magnitude; i.e.,

$$G = A + B \ . \tag{13}$$

Similarly, evaluating the pressures at the y = d interface gives

$$C + D = C\,(1 + V) = A\,e^{-i\alpha_2 d} + B\,e^{i\alpha_2 d} \ . \tag{14}$$

Dividing Equation (13) by Equation (14) gives

$$T = \frac{G}{C} = \frac{(1 + \frac{B}{A})(1 + V)}{e^{-i\alpha_2 d} + \frac{B}{A}\,e^{i\alpha_2 d}} \ . \tag{15}$$

Substitution of $\frac{B}{A}$ from Equation (4) and V from Equation (11) into Equation (15) gives

$$T = \frac{4Z_1Z_2}{(Z_1 - Z_2)(Z_2 - Z_3)\,e^{i\alpha_2 d} + (Z_1 + Z_2)(Z_2 + Z_3)\,e^{-i\alpha_2 d}} \ . \tag{16}$$

In the foregoing discussion transmission and reflection coefficients were developed, making no mention of attenuation within the layer. In most baffle materials absorption is present, and should be accounted for in the reflection and transmission coefficients. The presence of absorption causes the impedances to be complex; the wave numbers k and the angles of refraction θ will in general be

complex for absorptive layers.[3] Reflection and transmission coefficients using complex wave numbers and impedances can be written in the form

$$V = \rho\, e^{i\phi} \quad \text{and} \quad T = \eta\, e^{i\phi} \,. \tag{17}$$

Using the notation

$$2\alpha_2 d = \alpha + i\beta \quad \text{and} \quad Z = \gamma + i\delta \,, \tag{18}$$

and applying the proper subscripts in Equation (16), expressions for the modulus and phase of T can be written.

If the media 1 and 3 are the same, which is true for a layer surrounded by water, then the phase and modulus of the transmission coefficient can be written

$$\eta^2 = \frac{16\,(\gamma_2^2 + \delta_2^2)(\gamma_1^2 + \delta_1^2)\, e^{-\beta} \left[1 + 2\rho_{12}^2\, e^{-\beta} \cos\,(2\phi_{12} + \alpha_2) + \rho_{12}^4 e^{-2\beta}\right]}{\left[(\gamma_1 + \gamma_2)^2 + (\delta_1 + \delta_2)^2\right]^2} \tag{19}$$

and

$$\phi = \frac{\alpha}{2} + A - B - C \tag{20}$$

where

$$A = \arctan \frac{\gamma_1\delta_2 + \delta_1\gamma_2}{\gamma_1\gamma_2 - \delta_1\delta_2} \,, \tag{21}$$

$$B = \arctan \frac{2(\gamma_1 + \gamma_2)\,(\delta_1 + \delta_2)}{(\gamma_1 + \gamma_2)^2 - (\delta_1 + \delta_2)^2} \,, \tag{22}$$

[3] For a discussion of transmission through absorbing media, see Reference 2, pp 52-54.

$$C = \arctan \frac{\rho_{12}^2 e^{-\beta} \sin (2\phi_{12} + \alpha)}{1 + \rho_{12}^2 e^{-\beta} \cos (2\phi_{12} + \alpha)} , \tag{23}$$

and

$$\rho_{12}^2 = \frac{(\gamma_1 - \gamma_2)^2 + (\delta_1 - \delta_2)^2}{(\gamma_1 + \gamma_2)^2 + (\delta_1 + \delta_2)^2} , \tag{24}$$

and

$$\phi_{12} = \arctan \frac{2 (\delta_1\gamma_2 - \delta_2\gamma_1)}{\gamma_1^2 - \gamma_2^2 + \delta_1^2 - \delta_2^2} . \tag{25}$$

The foregoing expressions give the transmittivity for a layer, and are equally applicable to a dome segment or a plane baffle. Using the appropriate physical constants Equations (19) and (20) combine to give T. These expressions are bulky and can be replaced by simplified equations for certain situations. For instance, if the attenuation losses in the layer are small, an approximate method can be used to describe the transmitted sound field.

There are three approximate methods[4] described in the literature which agree closely with the exact theory for thin metal plates. Each of these methods was used to generate transmittivities for a range of incidence angles and frequencies. Representative results of these calculations are shown in Figures A2.1.2 to A2.1.13. Reissner's method[5] is seen to give good results over a wide frequency range. This method is used for subsequent computation of transmittivities through the dome.

For a sample solution, a curved dome was considered having an elliptical shape. A plane wave incident at the trailing edge was assumed to propagate parallel to the major axis. The dome was

[4] See References 4, 5, 6, and 7.

[5] A presentation appears in Reference 7.

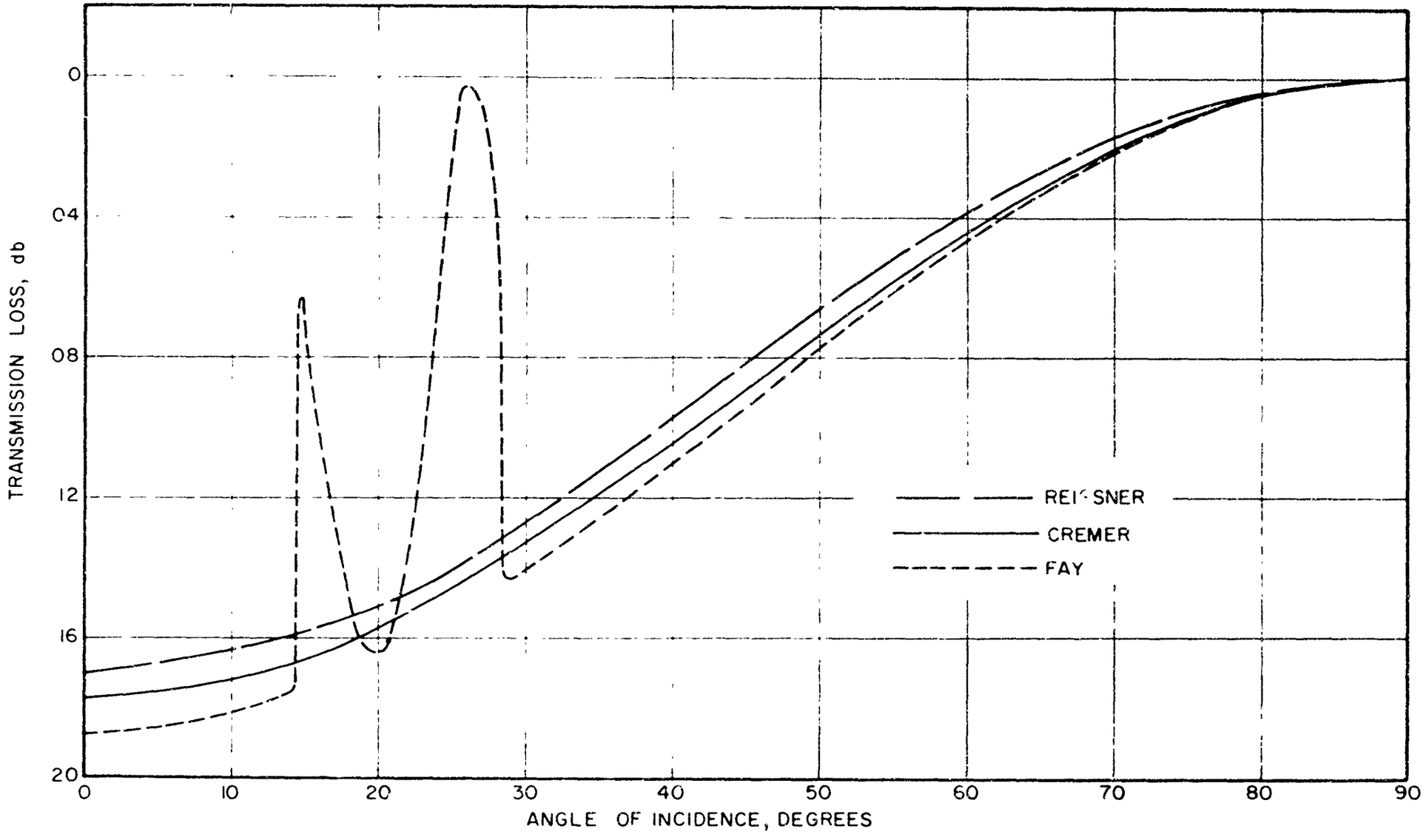

Fig. A2.1.2 – TRANSMISSION LOSS FOR 1/2" FLAT STEEL PLATE IN WATER AT f = 1KC

TEXAS RESEARCH ASSOCIATES
AUSTIN, TEXAS
DWG 2000-3
9-7-61
FG MM

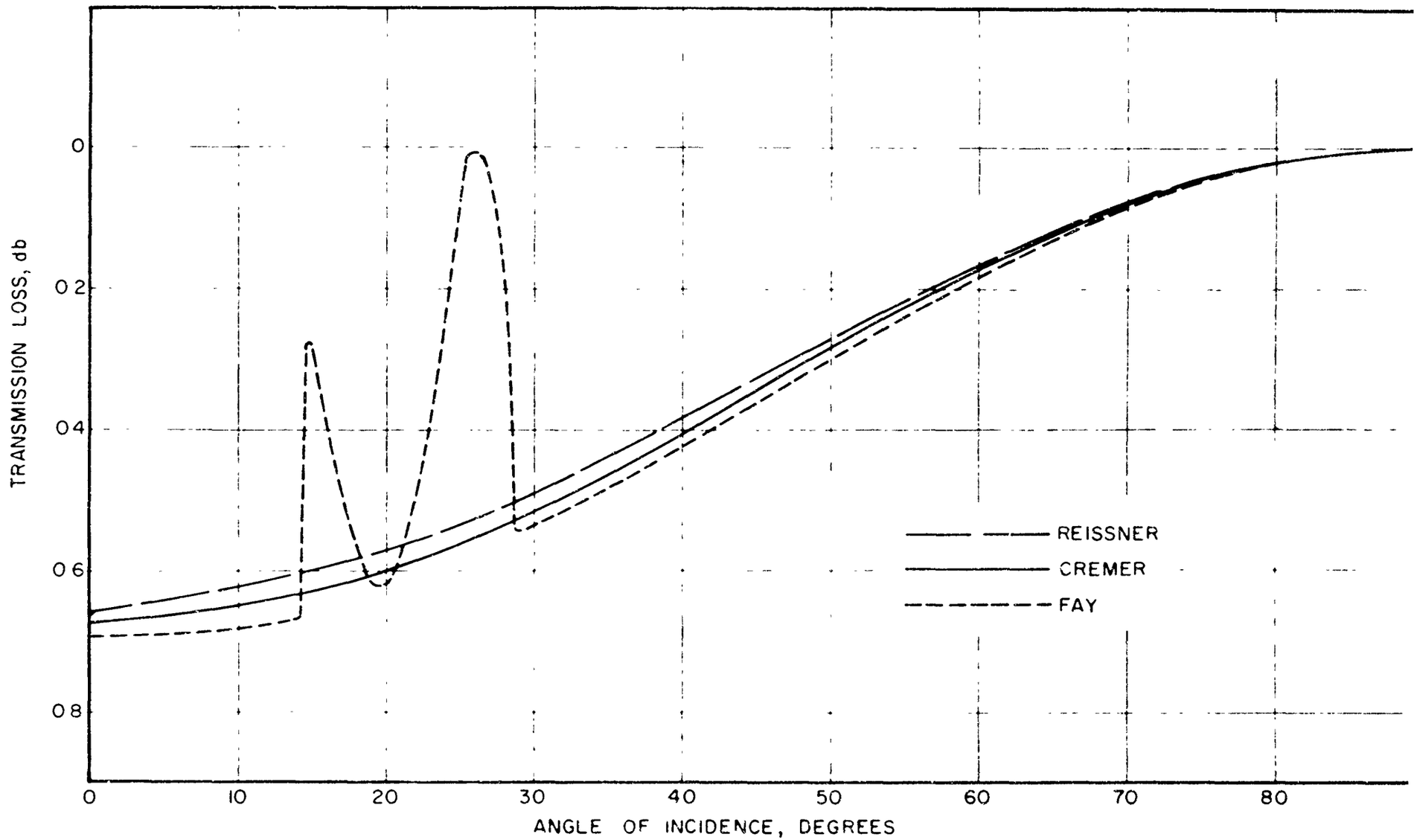

Fig. A2.1.3- TRANSMISSION LOSS FOR 1/2" FLAT STEEL PLATE IN WATER AT f = 2 KC

TEXAS RESEARCH ASSOCIATES
AUSTIN, TEXAS
9-7-61
DWG 2000-4
FG MM

TEXAS RESEARCH ASSOCIATES
9-7-61
MM

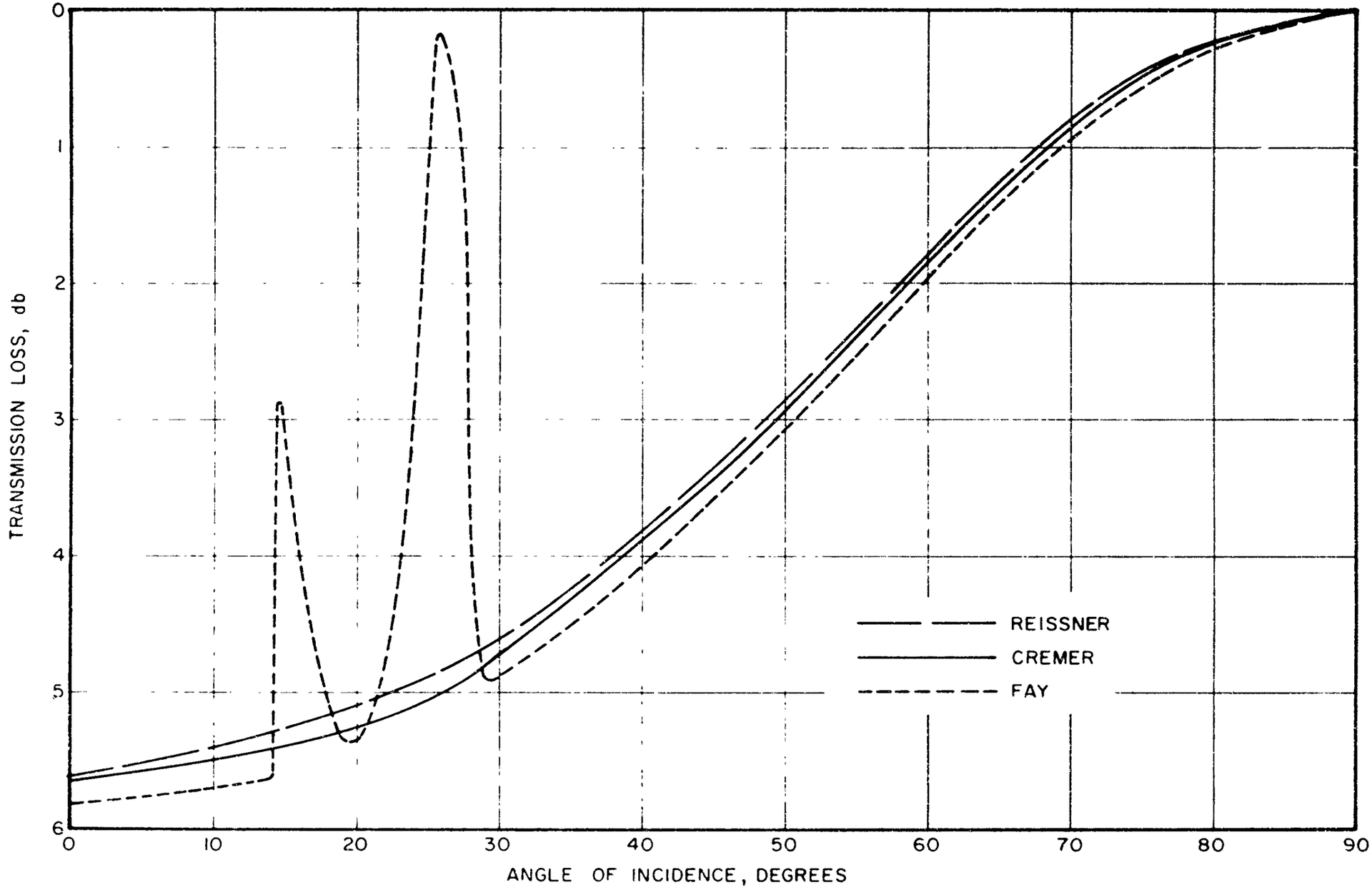

Fig. A2.1.4 - TRANSMISSION LOSS FOR 1/2" FLAT STEEL PLATE IN WATER AT f = 8 KC

TEXAS RESEARCH ASSOCIATES
AUSTIN, TEXAS
9-7-61
DWG 2000-2
FG JRR

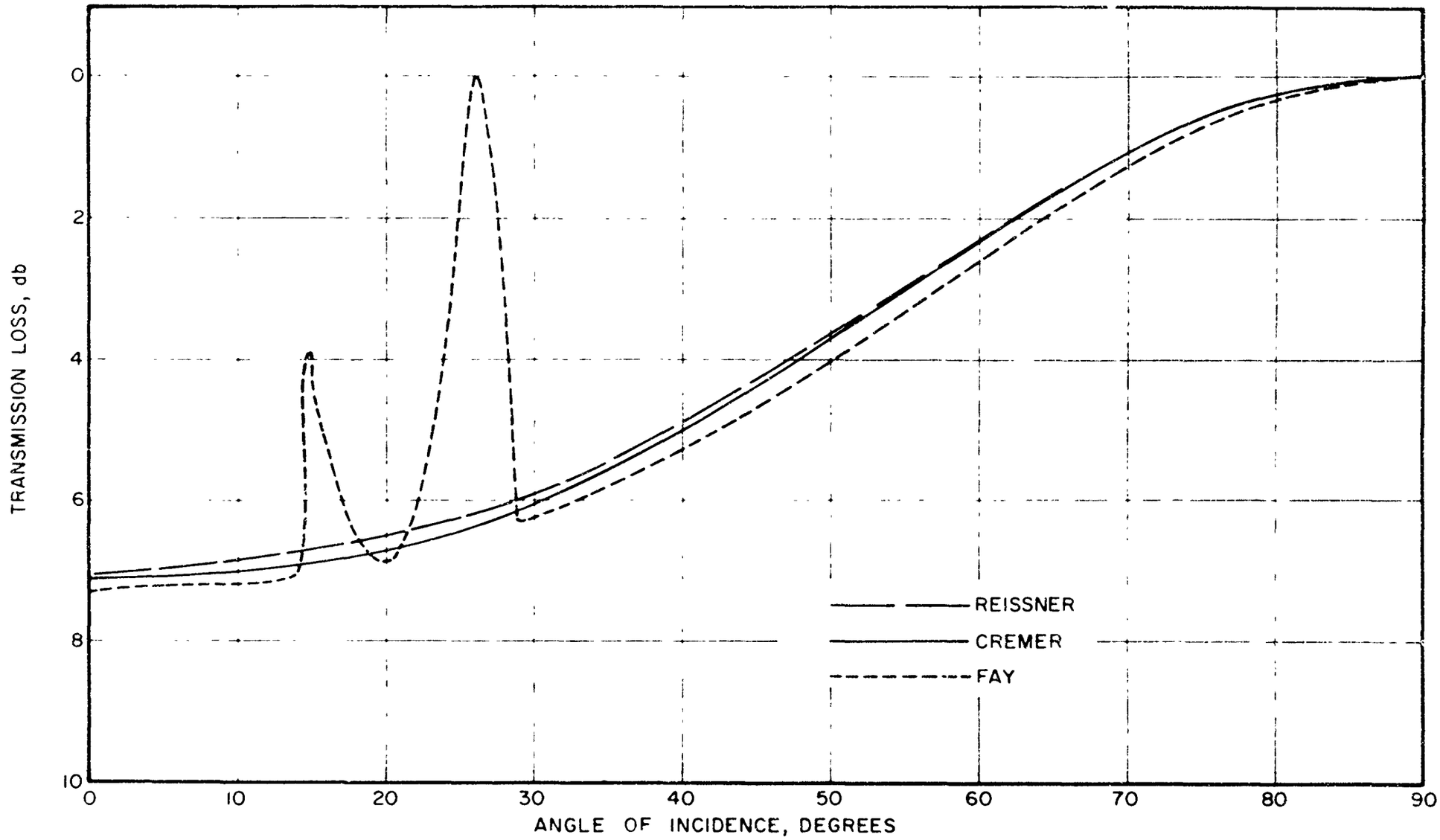

Fig. A2.1.5-TRANSMISSION LOSS FOR 1/2" FLAT STEEL PLATE IN WATER AT f = 10KC

TEXAS RESEARCH ASSOCIATES
AUSTIN, TEXAS
9-7-61
DWG 2000-1
FG MM

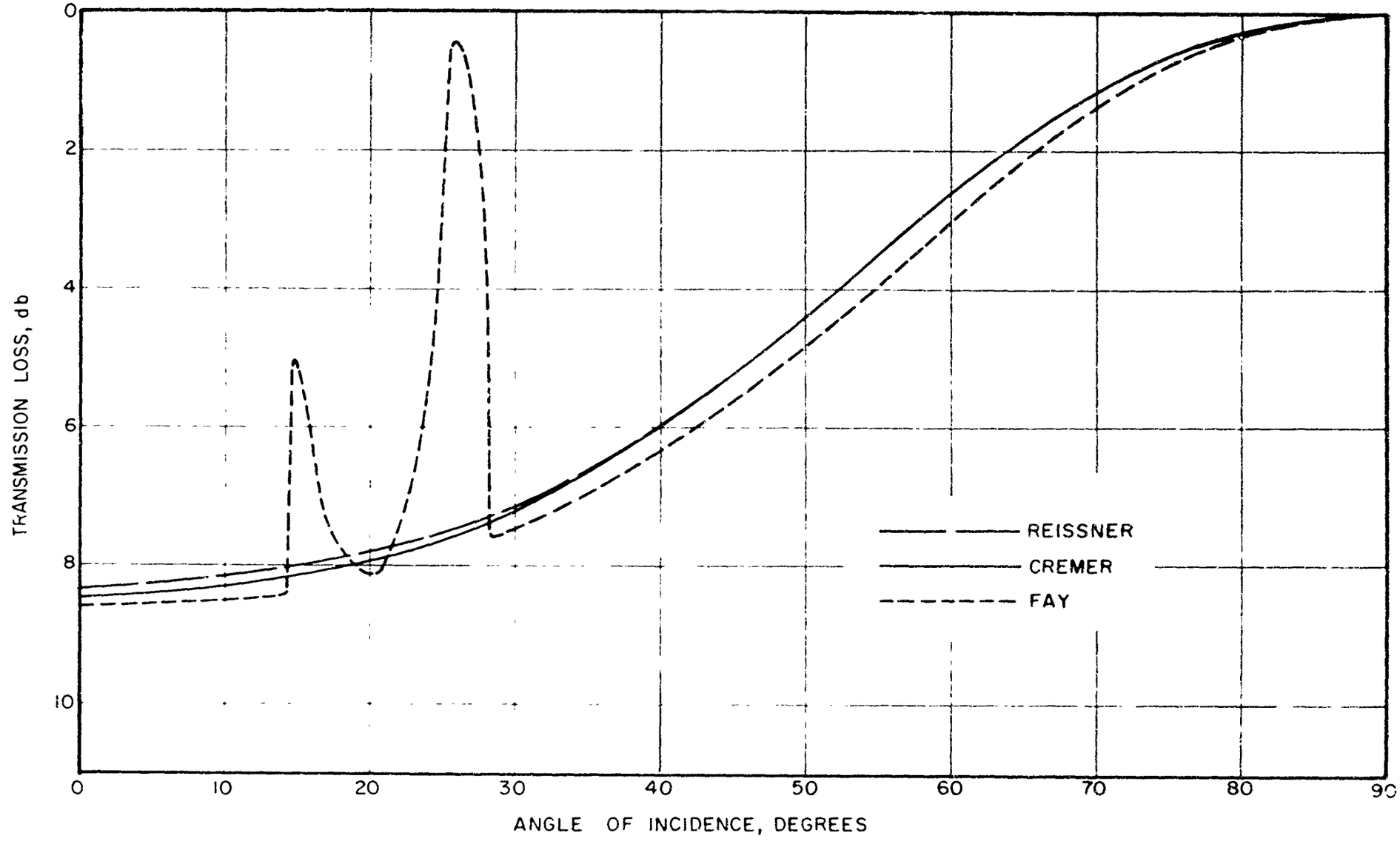

Fig. A2.1.6 - TRANSMISSION LOSS FOR 1/2" FLAT STEEL PLATE IN WATER AT f = 12KC

TEXAS RESEARCH ASSOCIATES
AUSTIN, TEXAS
9-7-61
DWG 2000-5
FG JRR

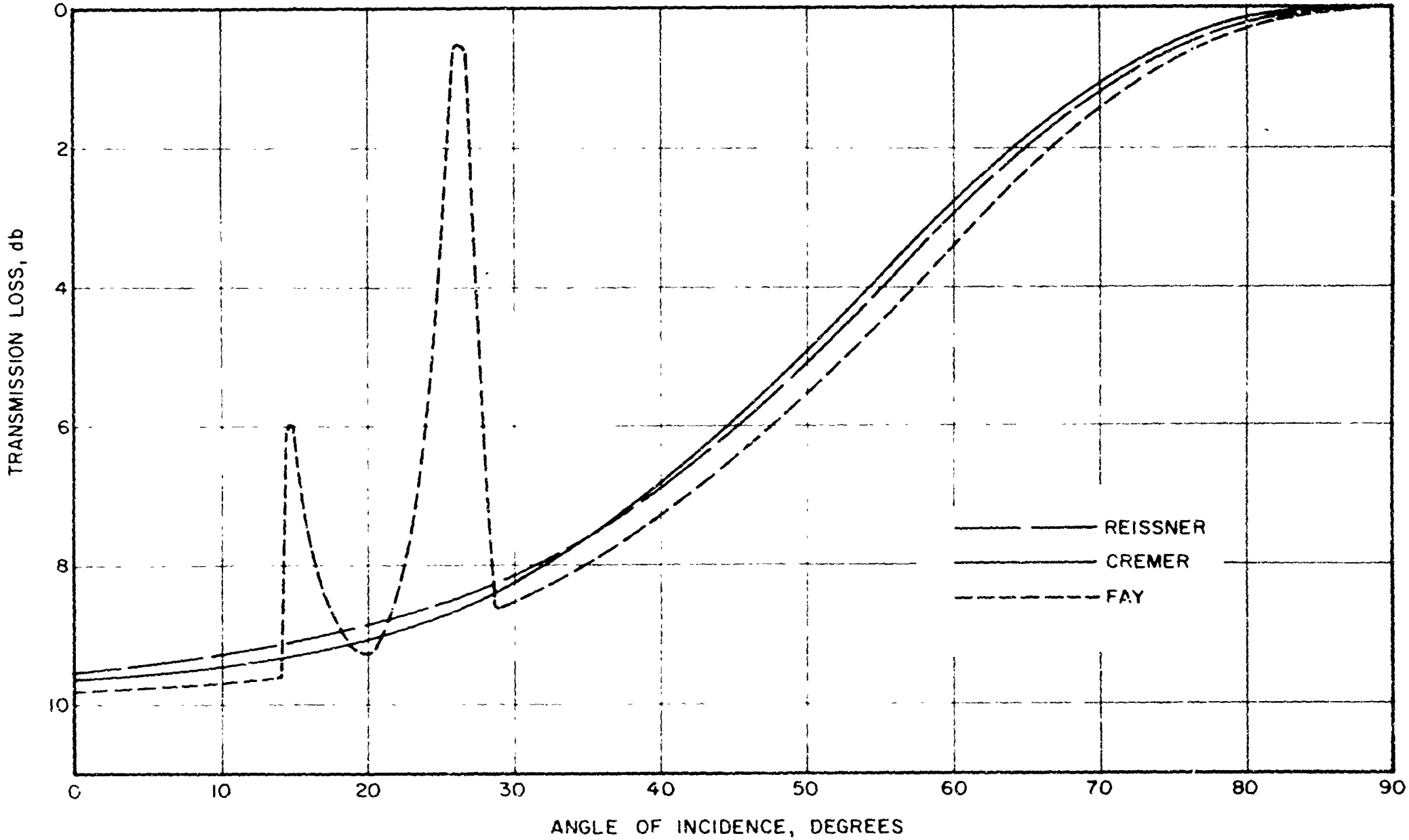

Fig.A2.1.7-TRANSMISSION LOSS FOR 1/2" FLAT STEEL PLATE IN WATER AT f = 14 KC

TEXAS RESEARCH ASSOCIATES
AUSTIN, TEXAS
9-7-61
DWG 2000-6
FG JRR

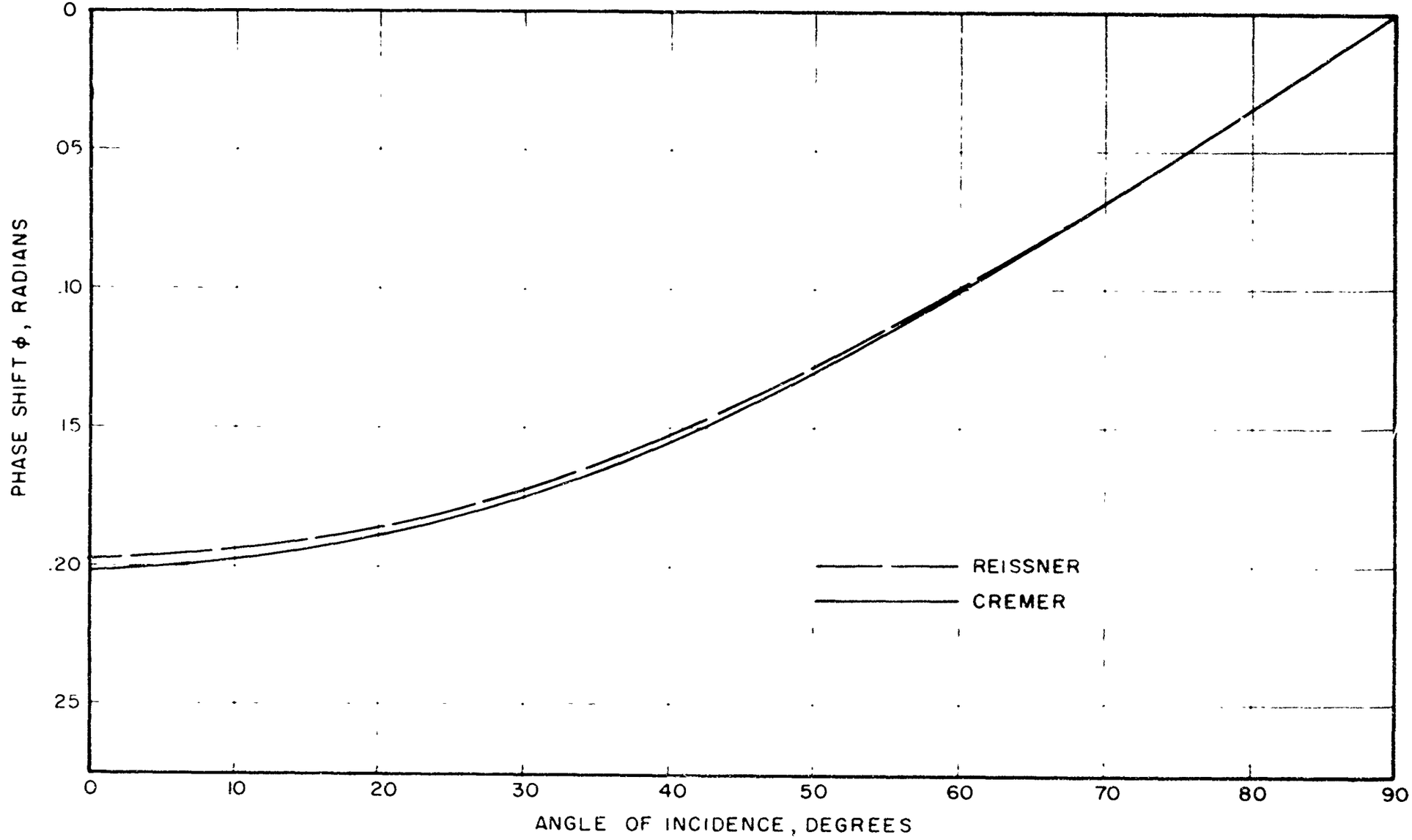

Fig. A2.1.8 – PHASE SHIFT FOR TRANSMISSION THROUGH 1/2" FLAT STEEL PLATE IN WATER AT f = 1KC

TEXAS RESEARCH ASSOCIATES
AUSTIN, TEXAS
9-7-61
DWG 2000-7 FG JRR

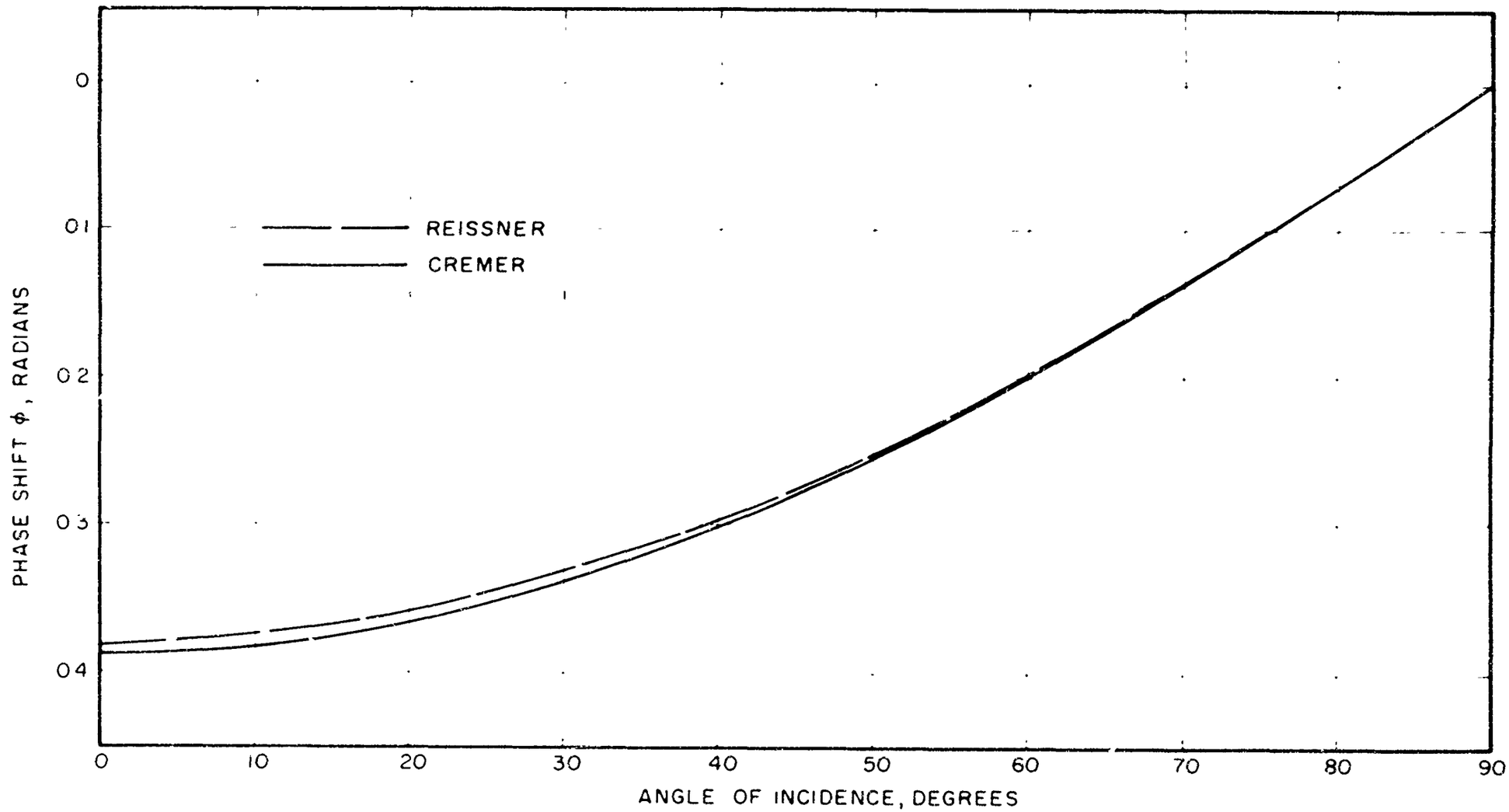

Fig. A2.1.9 — PHASE SHIFT FOR TRANSMISSION THROUGH 1/2" FLAT STEEL PLATE IN WATER AT f = 2KC

TEXAS RESEARCH ASSOCIATES
AUSTIN, TEXAS
9-7-61
DWG 2000-8
F.G. JRP

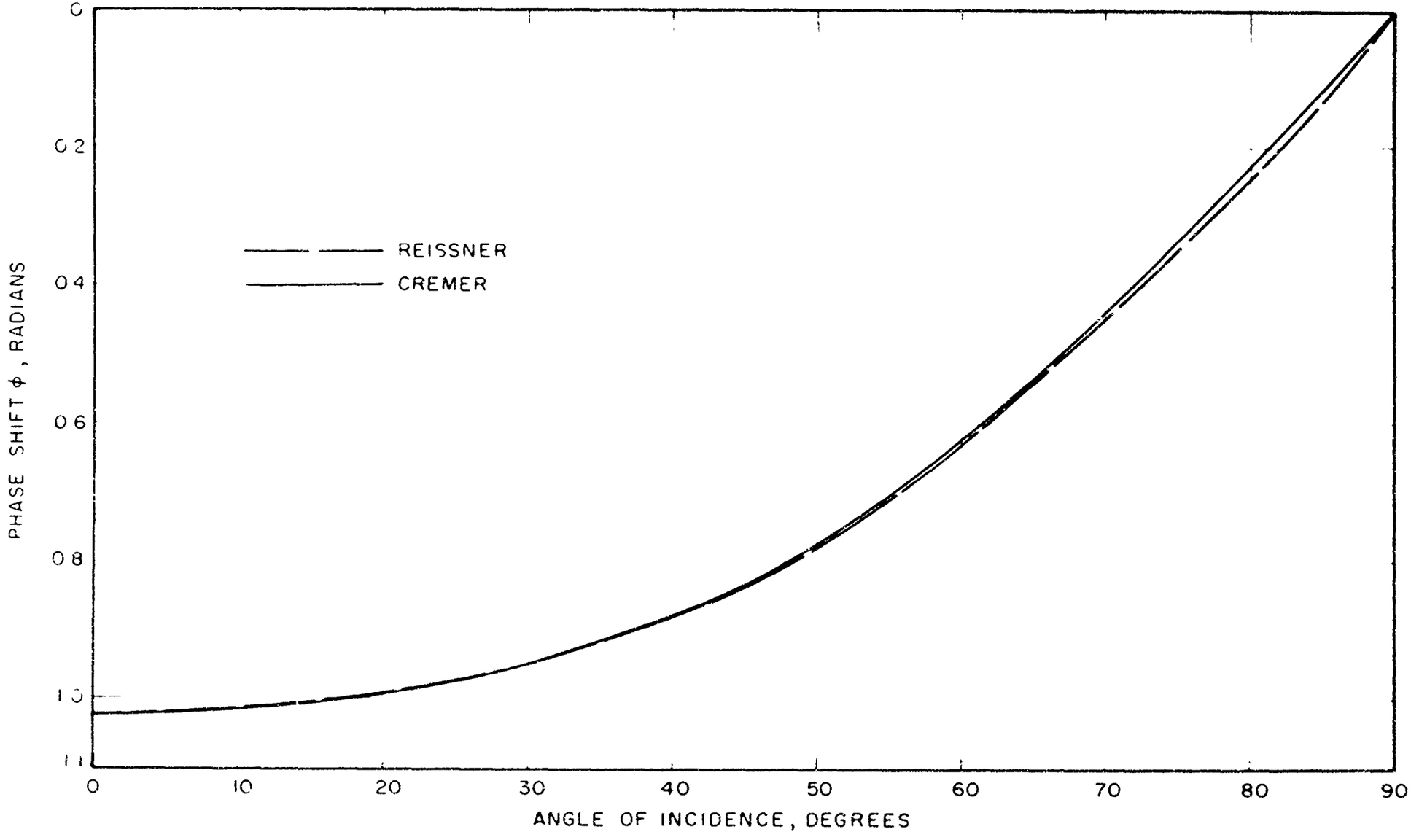

Fig. A2.1.10 – PHASE SHIFT FOR TRANSMISSION THROUGH 1/2" FLAT STEEL PLATE IN WATER AT f = 8 KC

TEXAS RESEARCH ASSOCIATES
AUSTIN, TEXAS
DWG 20[illegible] 9 7 61

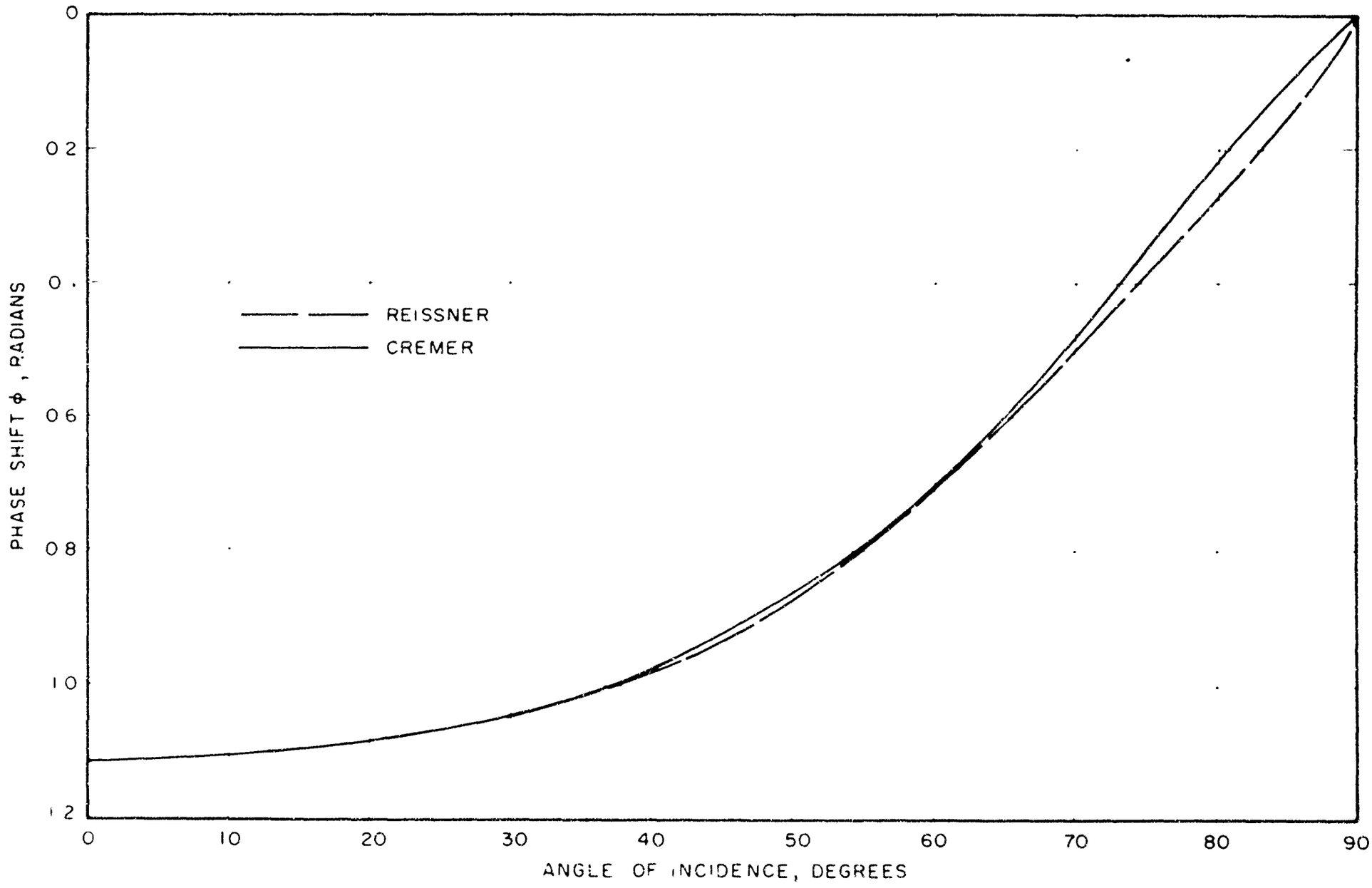

Fig.A2.1.11—PHASE SHIFT FOR TRANSMISSION THROUGH 1/2" FLAT STEEL PLATE IN WATER AT f = 10 KC

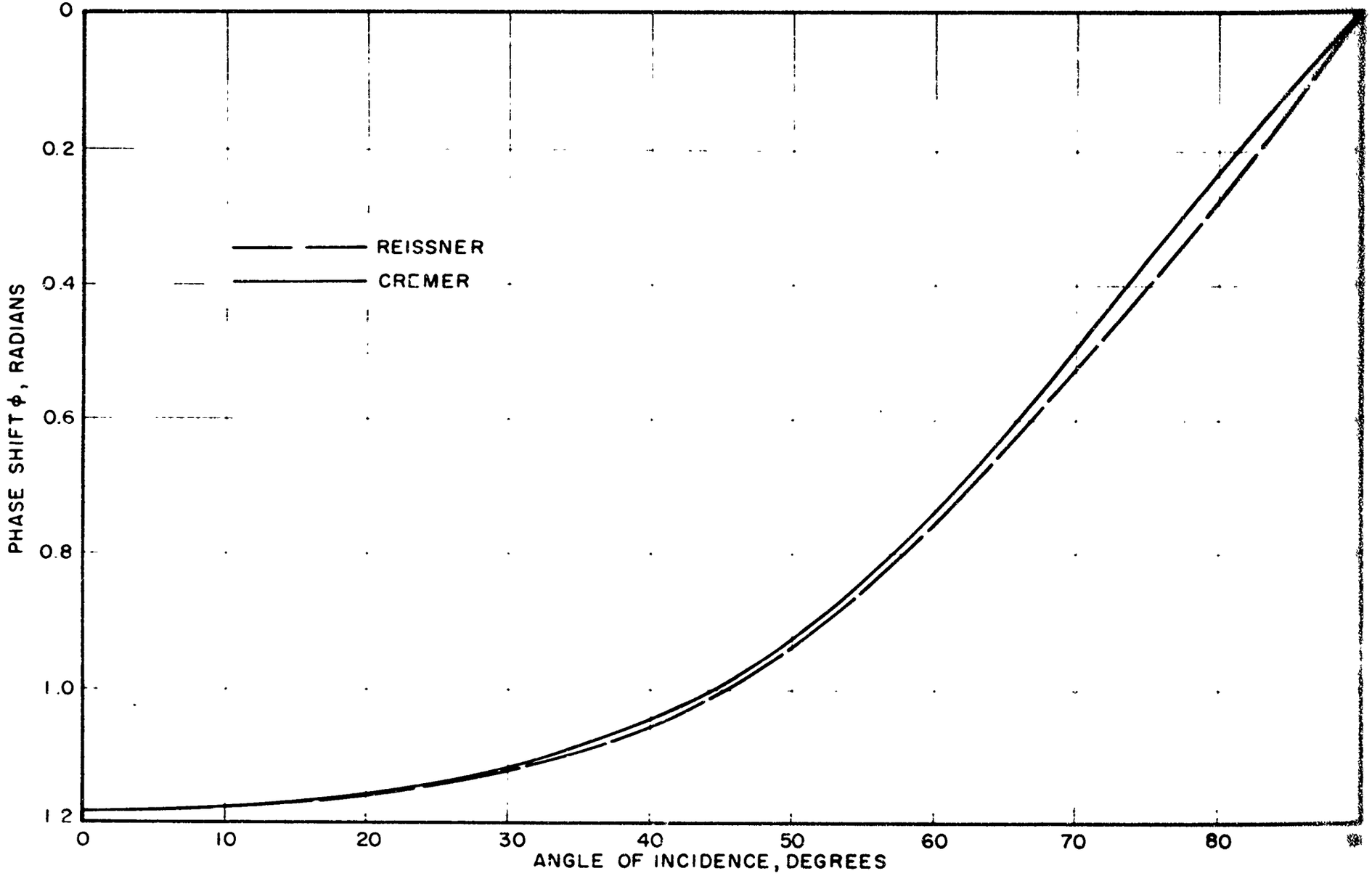

Fig.A2.1.12– PHASE SHIFT FOR TRANSMISSION THROUGH 1/2" FLAT STEEL PLATE IN WATER AT f = 12 KC

TEXAS RESEARCH ASSOCIATES
AUSTIN, TEXAS
9-7-61
DWG 2000-11 FG JRR

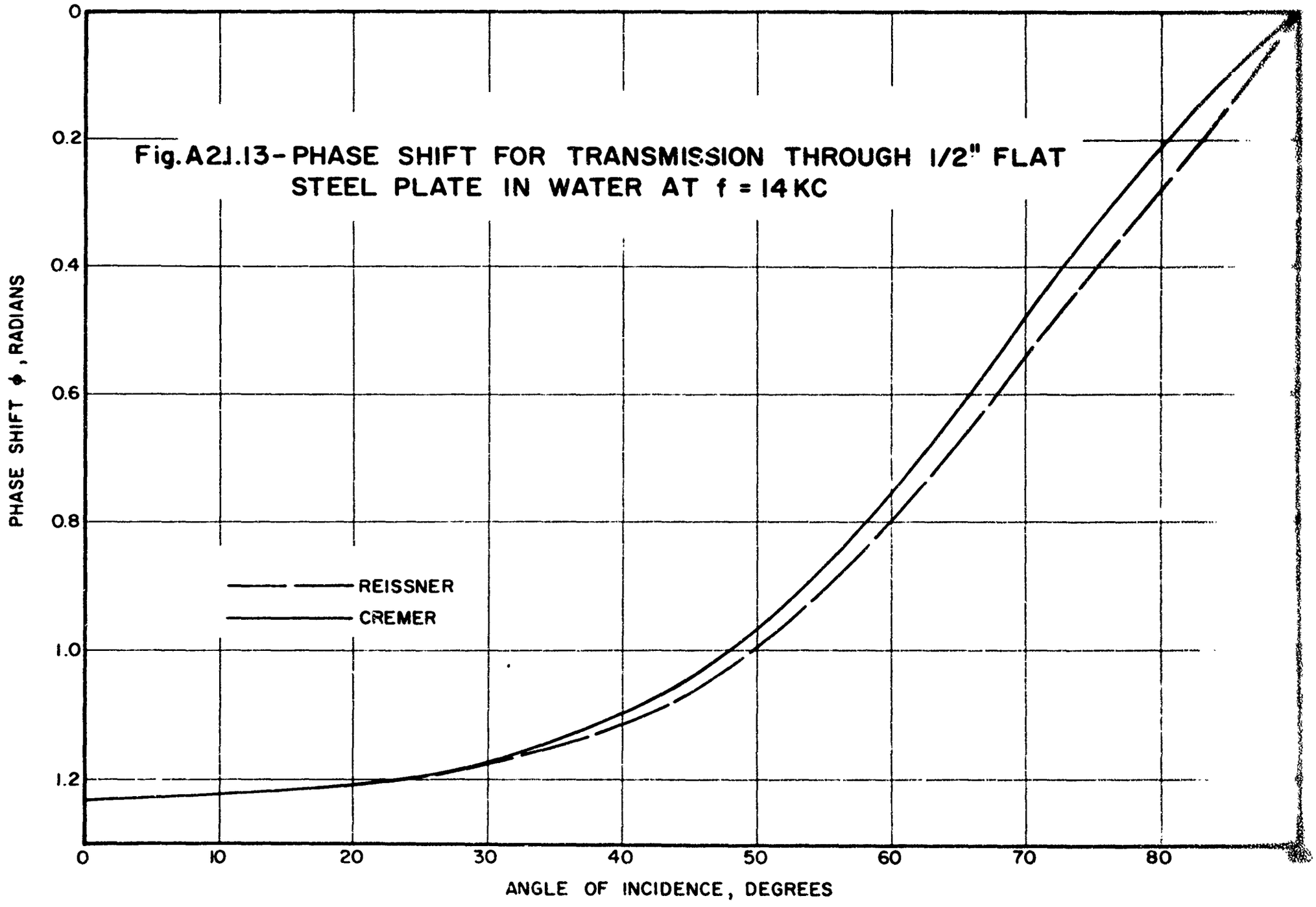

TEXAS RESEARCH ASSOCIATES
AUSTIN, TEXAS
9-7-61
DWG 2000-12
FG JRR

approximated by flat plate sections. The normalized transmitted pressure and phase shift relative to the incident wave were computed using Reissner's method for several frequencies. The resulting sound distributions are presented graphically in Figures A2.1.14 to A2.1.19.

This approximating technique can be applied equally well to other dome shapes to compute the transmitted pressure amplitude and phase. These calculations are of interest in determining the effect of the dome on the spatial extent of a noise source as it is seen by the baffle.

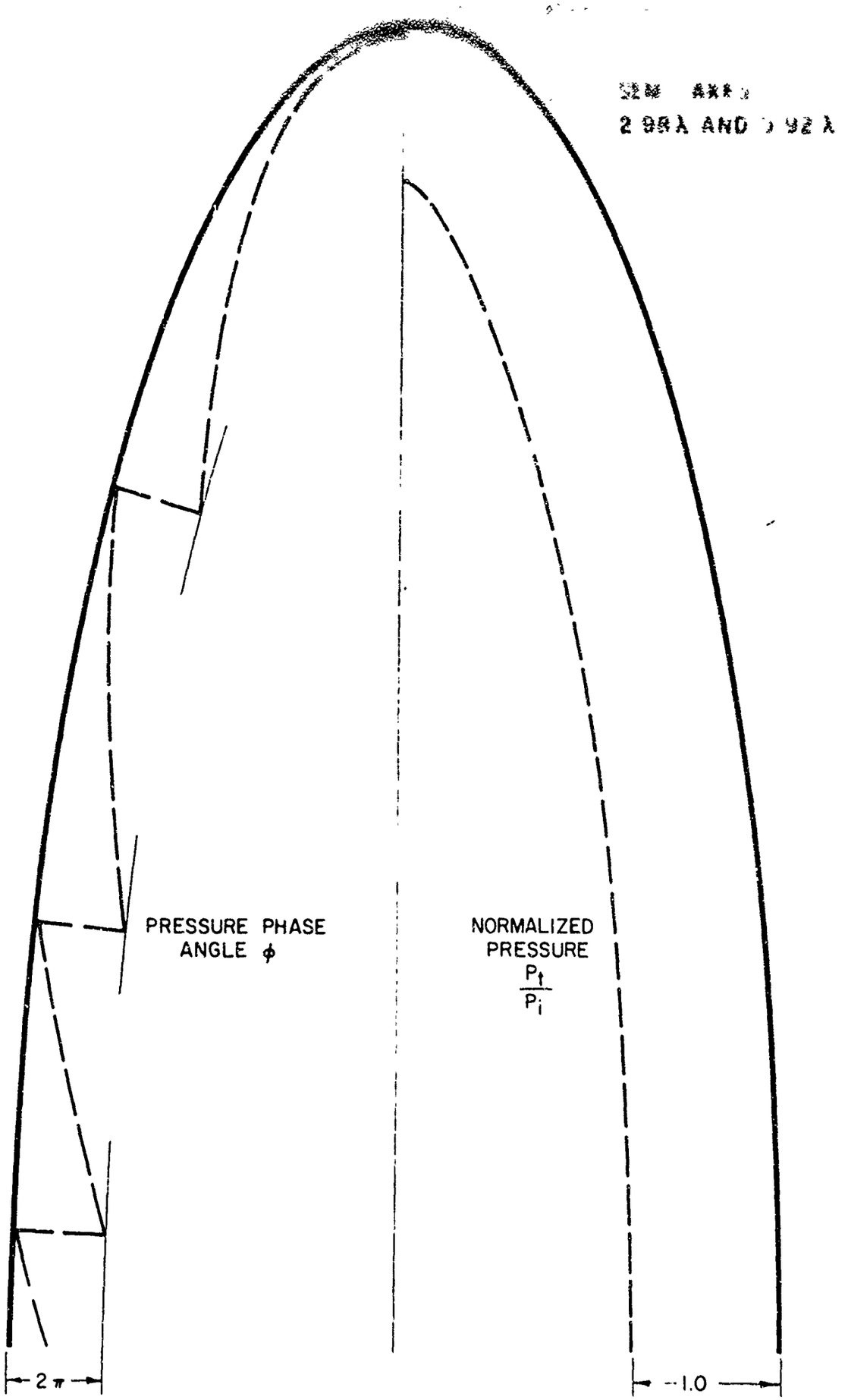

Fig.A2.1.14 - TRANSMISSION DATA INSIDE ELLIPTICAL 1/2" STEEL DOME FOR 1KC

TEXAS RESEARCH ASSOCIATES
AUSTIN, TEXAS 9-7-61
DWG 2000-15 FG-MM

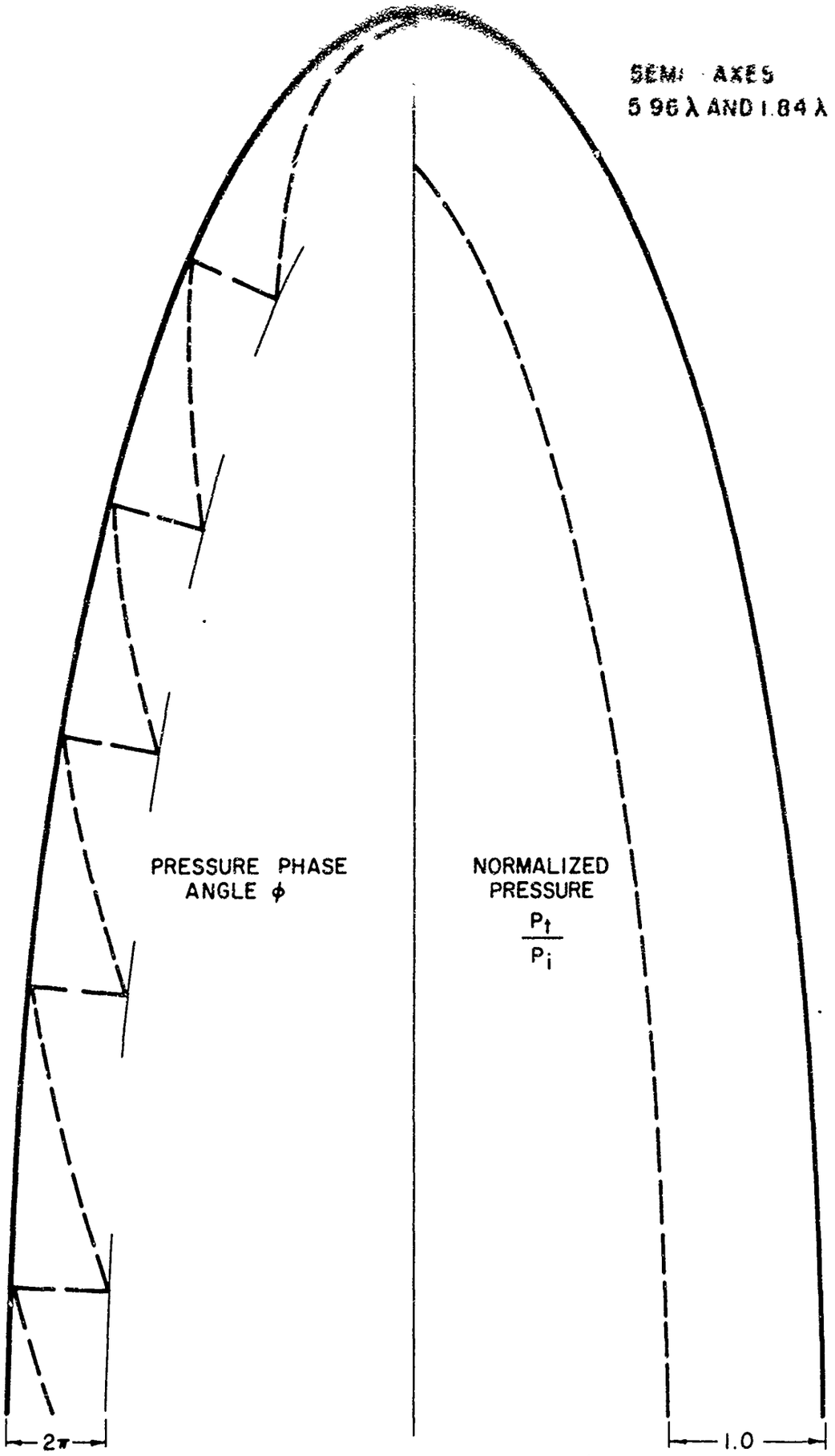

Fig. A2.1.15 - TRANSMISSION DATA INSIDE ELLIPTICAL 1/2" STEEL DOME FOR 2KC

TEXAS RESEARCH ASSOCIATES
AUSTIN, TEXAS 9 - 8 - 61
DWG 2000 - 16 FG MM

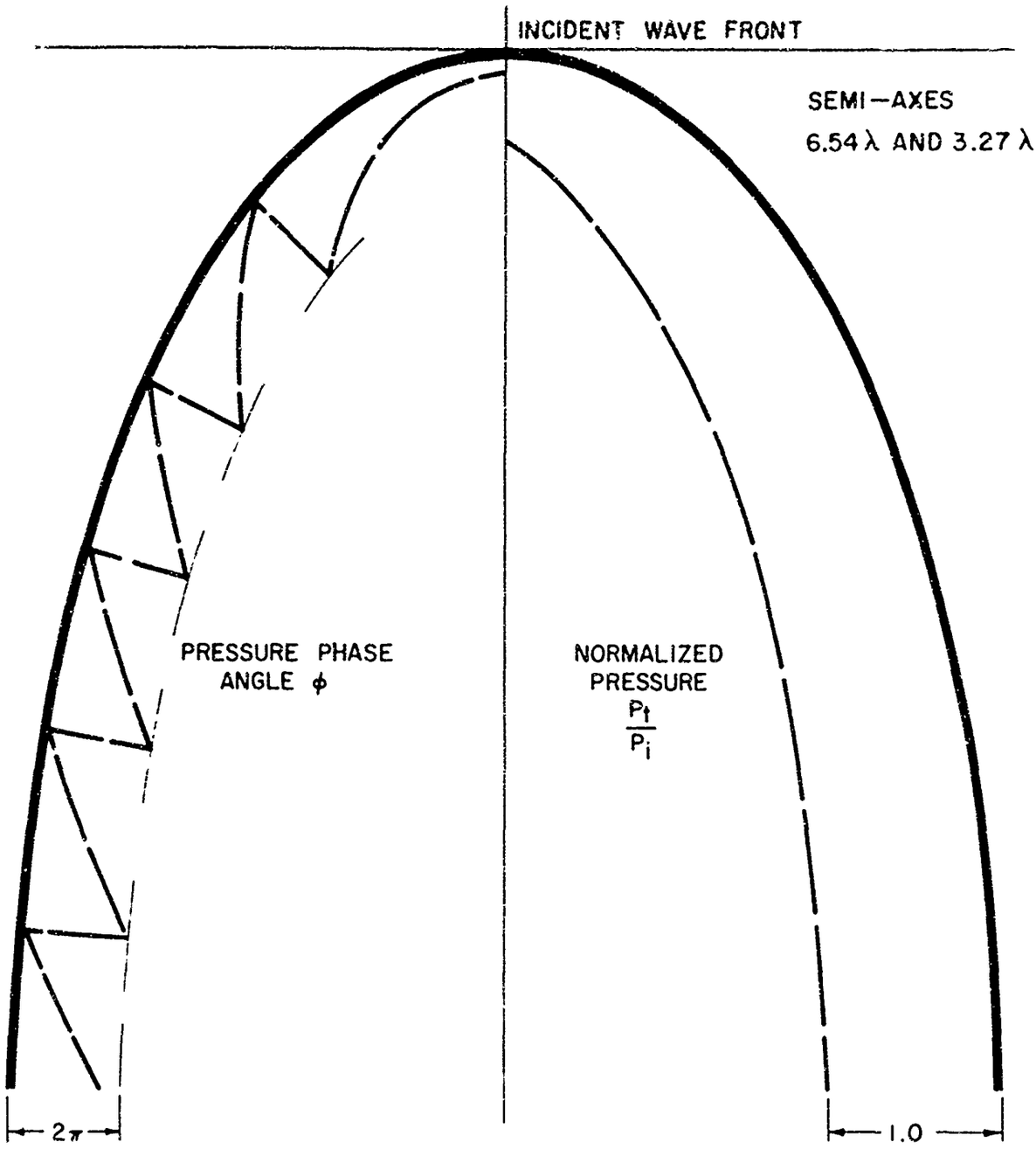

Fig. A2.1.16 – TRANSMISSION DATA INSIDE ELLIPTICAL 1/2" STEEL DOME FOR 8KC

TEXAS RESEARCH ASSOCIATES
ALSTIN, TEXAS 9 - 8 - 61
DWG 2000-17 FG MM

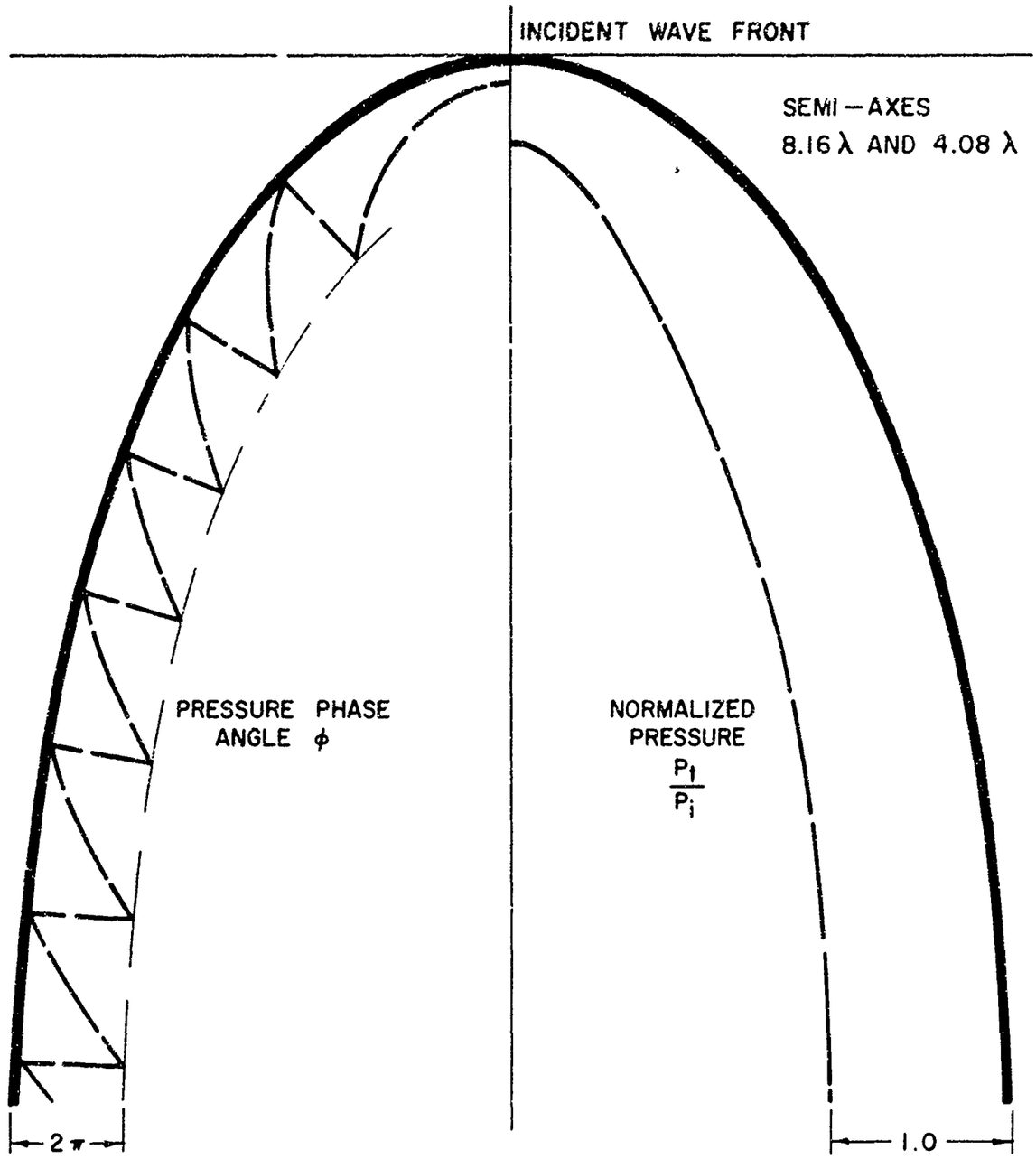

Fig. A2.1.17 - TRANSMISSION DATA INSIDE ELLIPTICAL 1/2" STEEL DOME FOR 10KC

TEXAS RESEARCH ASSOCIATES
AUSTIN, TEXAS 9 – 8 – 61
DWG 2000 - 18 FG MM

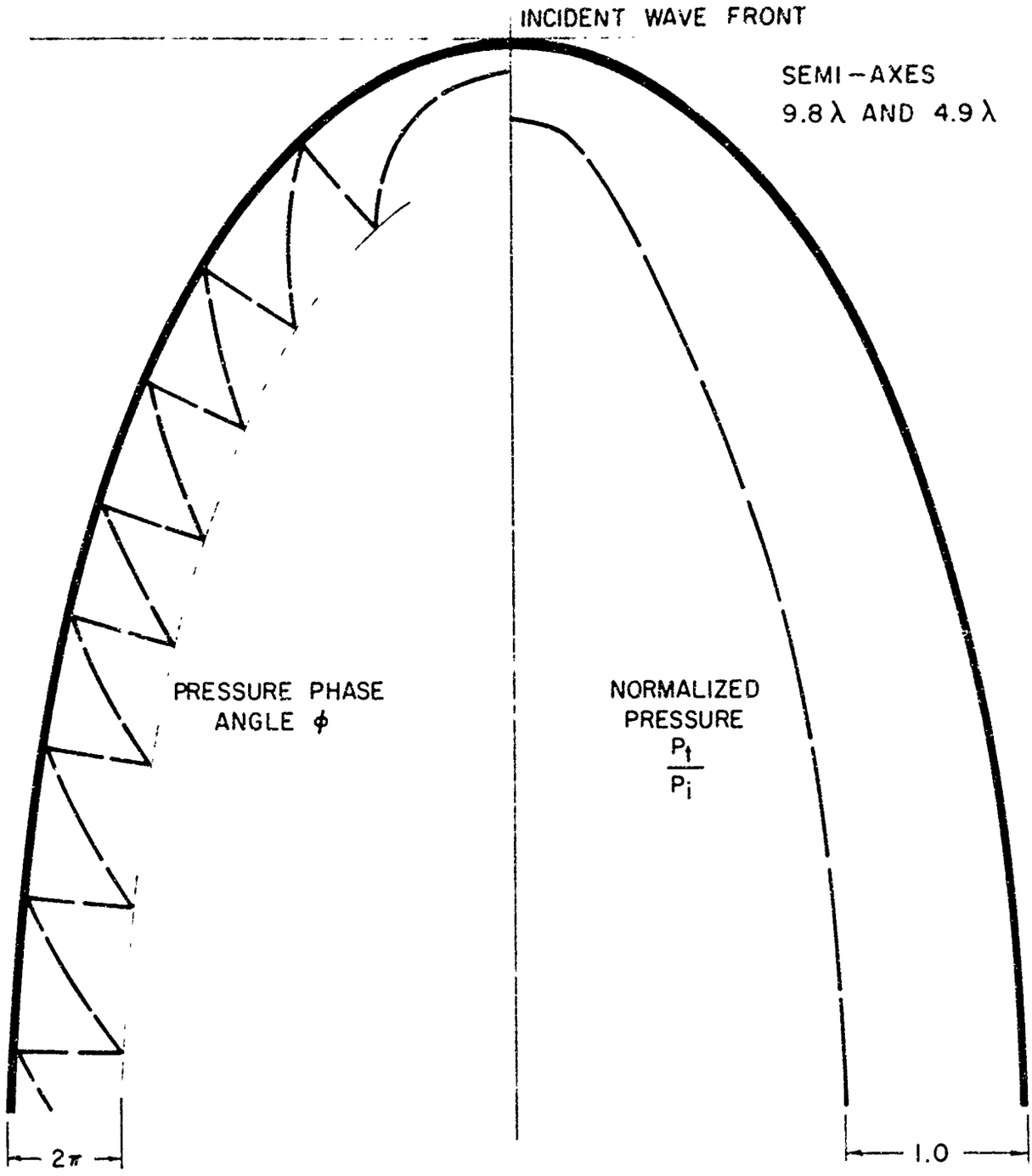

Fig. A 2.1.18 - TRANSMISSION DATA INSIDE ELLIPTICAL 1/2" STEEL DOME FOR 12 KC

TEXAS RESEARCH ASSOCIATES
AUSTIN, TEXAS 9-8-61
DWG 2000-19 FG MM

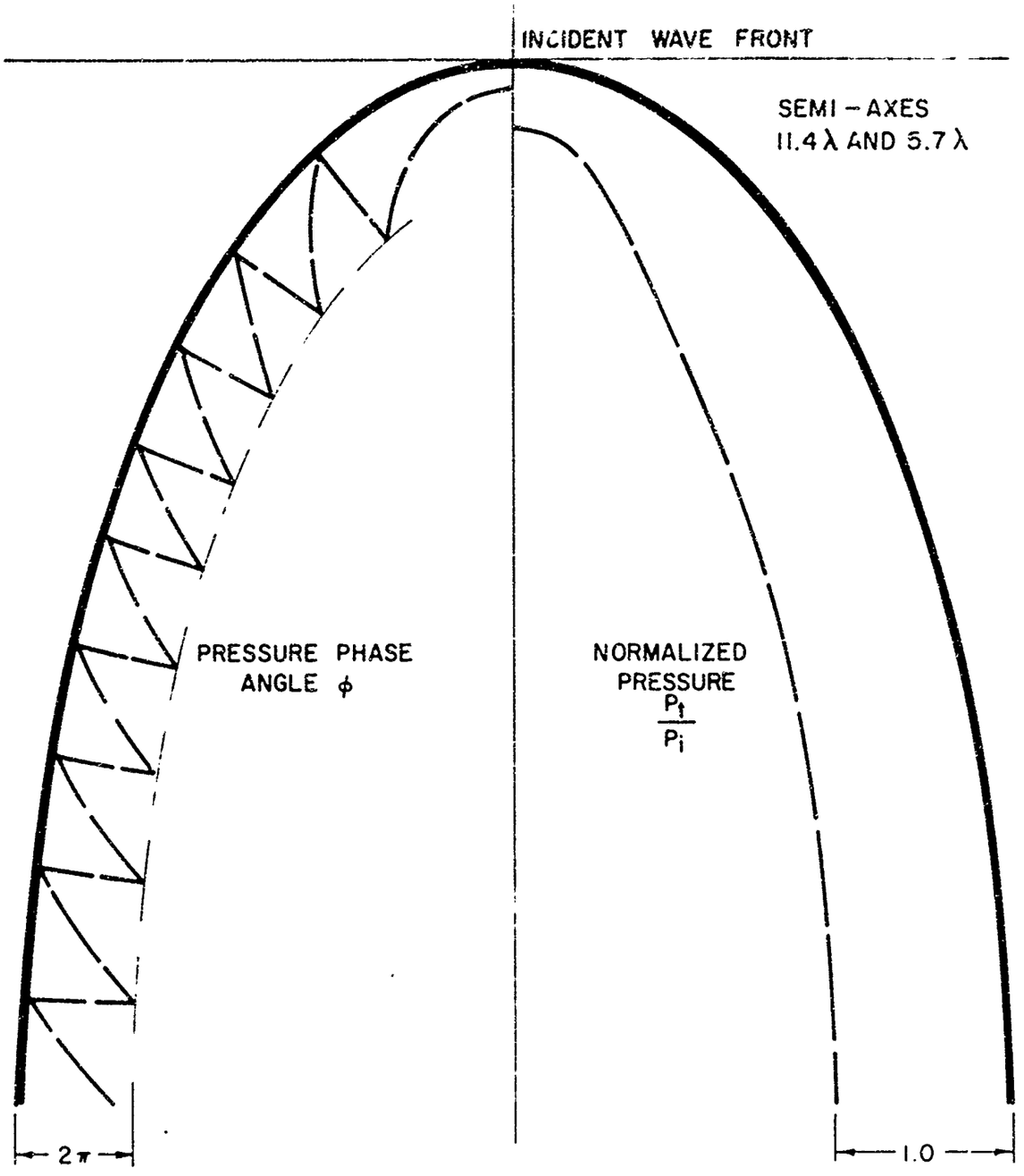

Fig. A2.1.19 - TRANSMISSION DATA INSIDE ELLIPTICAL 1/2" STEEL DOME FOR 14 KC

TEXAS RESEARCH ASSOCIATES
AUSTIN, TEXAS 9 - 8 - 61
DWG 2000-20 FG MM

2.2 The Transmission of Sound Through Sonar Baffles

If data are given to supply the physical constants of Equation (18), the transmittivity for the particular layer is calculable using Equations (19) and (20). In Equation (18) the term β represents the total attenuation for the layer thickness. Inspection of Equation (19) indicates that the transmittivity modulus is diminished for increasing β. The effect of increased β increases the phase angle as evidenced by Equations (20) and (23). Both these mathematical predictions are intuitively agreeable.

There are occasions which warrant the effort to determine transmittivity according to Equations (19) and (20). For instance, if the field between the baffle and transducer is to be processed for display, the pressure magnitude and phase are needed. These require solution giving pressure amplitude and phase. However, at other times the transmittivity magnitude alone is sufficient. This situation can be handled by noting the diffraction level, behind the proposed baffle and then determining the baffle thickness needed to attenuate the transmitted energy to below this level. Such design information can be generated using the material attenuation characteristics in db loss/inch versus frequency.[6]

A logical extension of the single layer baffle is the multilayer composite baffle. This type baffle combines the advantages of interface reflectivities and attenuation to produce frequency band pass characteristics.[7] No expression is included here for multilayer transmittivities but these are described in the literature.[8]

The same technique and transmittivity equations for the simple baffle apply to the composite baffle. The over-all multilayer

---

[6] For example, see Reference 3.

[7] See, for example, Reference 1, p 85.

[8] For a discussion see Reference 2, p 59.

transmittivity expression takes the form of a product of terms representing transmittivities of the individual layers.[9] However, for design evaluation purposes it seems desirable to have the freedom of viewing individual layer effects separately; also this allows the freedom of studying the effects of various orders of layer combinations without completely solving a new baffle each time. Therefore, it is at this point intended to successively apply the results of Equations (19) and (20) for solving multi-layer transmittivities. The over-all transmission coefficient is the product of the moduli and the phase is the sum of the phases for the respective layers.

[9] Ibid.

REFERENCES FOR APPENDIX 2

1. Lindsay, R. B., Mechanical Radiation, New York: McGraw-Hill. 1960.

2. Brekhovskikh, L. M., Waves in Layered Media. New York: Academic Press, 1960.

3. Goodrich, B. F., Aerospace and Defense Products Division, "Products-Materials for Underwater Sound Applications," Second Edition, Akron 18, Ohio (July 1961).

4. Fay, R. D., "Notes on Transmission of Sound Through Plates," J. Acoust. Soc. Am. 25, 220-223 (1953).

5. Reissner, H., "The Vertical and Oblique Passage of a Flat Compression Wave, Produced in a Liquid, Through a Plane-Parallel Plate Placed in the Liquid," Helv. Phys. Acta 11, 140-145 (1938).

6. Cremer, L., "Theorie der Schalldampfung durch Wande bei schrogem Einfall," Akust. Z. 7, 81-104 (1942).

7. Thurston, G. B., and Stern, R.,"Computation of Acoustic Transmission Through a Plane Elastic Plate." Report 2784-3-T, Willow Run Laboratories, The University of Michigan (October 1959).

8. Goodman, R. R., and Stern, R., "The Transmission of Sound by a Hemispherical Shell Mounted on a Rigid Plate," J. Acoust. Soc. Am. 34, 338-344 (1962).